








Research Article

Petrology, Geochemistry and Petrogenesis of the Dykes from the Zhob Ophiolite, Pakistan

Abdul Naeem^{1,2}, Muhammad Ayoub Khan^{2*}, Andrew Craig Kerr³, Muhammad Panezai², Muhammad Tariq⁴

¹Geological Survey of Pakistan, Quetta, Pakistan

²Center of Excellence in Mineralogy, University of Balochistan, Quetta, Pakistan

³School of Earth and Environmental Sciences, Cardiff University, Cardiff, Wales CF10 3YE, UK

⁴National Centre of Excellence in Geology, University of Peshawar, Pakistan

*Corresponding author: ayoub.cemuob@gmail.com

Article History:

Received:
2 July 2024
Revised:
5 December 2024
Accepted:
2 January 2025
Published online:
24 June 2025
Published in Issue:
30 June 2026

Abstract

The highly deformed Zhob ophiolite comprises the Ali Khanzai, Naweoba, and Omzha blocks. Each of these blocks contains both felsic and mafic dyke swarms. The felsic dykes occur as patches and pods in gabbroic bodies of crustal sections while mafic dykes crosscut the mantle peridotite of these blocks. Felsic dykes are plagiogranite and are composed of quartz, plagioclase and accessory ferromagnesian minerals whereas mafic dykes are basaltic in composition and contain largely plagioclase, clinopyroxene, and hornblende with minor quartz grains. Major, trace and rare earth elements have been analyzed in the felsic and mafic to assess the tectonomagmatic setting of the Zhob ophiolite. The felsic dykes are calc-alkaline oceanic plagiogranites while mafic dykes are tholeiitic in composition. Chondrite normalized patterns for the felsic dykes are characterized by low values of the REEs and positive Eu anomalies which indicate that they were formed by partial melting of basic rocks under hydrous conditions. The mafic dykes show very slight Nb depletion and enrichment in large ion lithophile elements (LILE) over high field strength elements (HFSE) which suggest that mafic dyke swarms are derived from an undepleted mantle source. Oceanic rocks with such characteristics are generally thought to have formed by processes involving a subduction zone component in the source region by fluids released from the subducting slab. These features suggest a subduction related setting which indicates an island arc, back arc or supra-subduction zone affinity for the formation of both felsic and mafic dykes of the Zhob ophiolite.

Keyword: Mafic and felsic dykes, plagiogranite, supra-subduction zone, Zhob ophiolite

©2026 the Author(s). Published by the OICC Press under the terms of the [CC BY 4.0, Creative Commons Attribution License](https://creativecommons.org/licenses/by/4.0/), which permits use, distribution and reproduction in any medium, provided the original work is properly cited.

Cite this article: Naeem, A., Ayoub Khan, M., Craig Kerr, A., Panezai, M. & Tariq, M., (2026). Iranian Journal of Earth Sciences, Petrology, geochemistry and petrogenesis of the dykes from the Zhob Ophiolite, Pakistan. 18(2): 221-246. <https://doi.org/10.57647/j.ijes.2025.16948>

1. Introduction

Ophiolites are fragments of oceanic lithosphere that have been obducted tectonically along continental margins during orogenic processes. An intact ophiolite has almost a

complete stratigraphy from mantle peridotite to crustal rocks (Robertson, 2002). Partial melting of peridotites produces mafic melt which forms the oceanic crust while the partial melting of the mafic rocks of oceanic crust under

hydrous conditions produces minor felsic rocks known as plagiogranites (Klein and Langmuir, 1987; Arndt et al., 2009; Korenaga, 2013; Yazdi et al., 2016; Salehpour et al., 2025; Elmi et al., 2025). Fractional crystallization of basaltic magma and partial melting of the mafic rocks have been proposed for the formation of the felsic and basaltic dyke swarms, respectively (Beccaluva et al., 1999; France et al., 2010; Wanless et al., 2010; Brophy and Pu, 2012). The Bela-Zhob Valley-Waziristan ophiolitic belt extends from south to north in Pakistan and demarcates the western boundary of the Indian plate with the Afghan block of Eurasian plate (Fig. 1a; Gansser, 1979). The Zhob Valley contains three ophiolites namely Khanozai, Muslim Bagh and Zhob Ophiolites (Fig. 1b). Studies suggest that the felsic and mafic dyke swarms of Waziristan and Muslim Bagh ophiolites (north and south of Zhob ophiolite, respectively) formed in a subduction-related setting (island arc, back arc basin and supra-subduction zone setting) (Khan et al., 2001; Kakar et al., 2014; Haghparast et al., 2019; Talebian Borojenie et al., 2025). The Zhob ophiolite contains three detached blocks: the Naweoba, Omzha and Ali Khanzai blocks (Fig. 1c, d, e), which are highly tectonised. It is therefore challenging to distinguish the different rock types in these deformed blocks. All blocks of Zhob Ophiolite contain ultramafic gabbros and volcanic rocks (Khan et al., 2020a, b; Naeem et al., 2021, 2022). These rocks were first reported as intrusive bodies by Jones (1961), however, prior to this study little petrographic data and no geochemistry was available on these rocks. In this study, we report the first detailed fieldwork, petrography and the first major and trace element geochemistry of the felsic and mafic dyke swarms from the Zhob ophiolite in Pakistan to determine the geologic and tectonic setting of the Zhob ophiolite and the origin of the dykes.

2. Geological Setting

The Zhob ophiolitic blocks are part of the Waziristan-Muslim Bagh ophiolites of Neo-Tethyan origin that represent the suture zone between the Indian plate and Afghan block (Fig.1; Ahmed and Abbas, 1979). The Waziristan ophiolite occurs in the north of the Zhob ophiolite and comprises crustal sections, well-exposed mantle sections and upper volcano-sedimentary units, that formed in a back-arc basin (Khan, 2000). In the south of the Zhob ophiolite, the Muslim Bagh ophiolite comprises mostly ophiolitic rock units including the crustal section, transition zone, mantle section, lava and metamorphic sole rocks in a back-arc basin setting and hosts chromitite, volcanogenic massive sulfide (VMS), and manganese deposits (Fig. 1; Kakar et al., 2014; Khan et al., 2020 a, b). Further to the south, the Bela ophiolite is found, and this was generated in a supra-subduction zone setting (Ahmed, 1991, 1993; Ashrafi et al., 2024). The Katwaz basin occurs

in the west of the Zhob ophiolite and is comprised of a thick sequence of shallow marine flysch sediments between the central Afghan block and Indian plate (Cassaigneau, 1979). Two tectonic blocks: the Zhob valley ophiolite and Katwaz basin are found between the Indian plate and Afghan block. The Zhob ophiolitic blocks in the Zhob Valley are divided into three tectono-stratigraphic rock units: 1) the flysch zone, 2) Zhob ophiolite and 3) the calcareous zone (Naeem et al., 2021, 2022; Nazari et al., 2023) with the Zhob ophiolite being thrust over the calcareous zone (Fig.1; Şengor, 1987; Kazmi and Jan, 1997). The Zhob ophiolitic blocks, known as the Naweoba, Ali Khanzai, and Omzha blocks (Jones, 1961) are further divided into six fault-bounded tectonostratigraphic units: a) Hyaloclastite-mudstone unit (Zhm), b) Basalt-chert unit (Zbc), c) Plutonic crustal rocks unit (Zpc), d) Mantle section rocks unit (Zms), e) Metamorphic rocks unit (Zmr), and f) Upper and lower sedimentary rocks unit (Zus and Zls) (Fig.1c,d,e; Naeem et al., 2021).

The rocks of the flysch zone were formed in a fluvial to shallow marine environment in a large sedimentary basin (Trelor and Izatt, 1993). The Nisai Formation of Eocene age unconformably overlies the Zhob ophiolitic blocks (Allemann, 1979). Felsic dyke rocks such as plagiogranite occur in the west of Naweoba, southwest of Ali Khanzai and southeast of Omzha blocks. The Naweoba block is the largest among these blocks with well exposed felsic and mafic dykes. The felsic dykes are found in the plutonic rocks as pods, lenses, and intrusions and occasionally crosscut the ultramafic rocks of Ali Khanzai block in contrast to the Naweoba and Omzha blocks. The Zhob ophiolitic blocks and their underlying and overlying rocks began to form and extend from the continental margin of the Indian subcontinent over the Neo- Tethys Ocean floor and obducted along with the Muslim Bagh ophiolite (Naeem et al., 2021). Studies on the petrography, geochemistry, geology and tectonic setting of the Zhob ophiolitic blocks and their comparison with Waziristan and Muslim Bagh ophiolite suggest that the Zhob ophiolite was also formed at the same time as the formation and emplacement of the Muslim Bagh ophiolite (Naeem et al., 2022).

3. Field Features of Felsic and Mafic Dykes

The felsic (plagiogranite) dykes of the Zhob ophiolite are intruded into the volcanic and plutonic mafic crustal rock units as lenses, pods, pockets, xenoliths and inclusions. The felsic dyke rocks (plagiogranite) are medium to coarse-grained, hard, compact and creamy white to white-green in colour, composed of quartz, plagioclase, apatite, zircon and accessory ferromagnesian minerals such as, biotite and magnetite. The intrusions of felsic dykes in the basal part of the gabbroic rocks in all blocks are common (Fig. 2a, b).

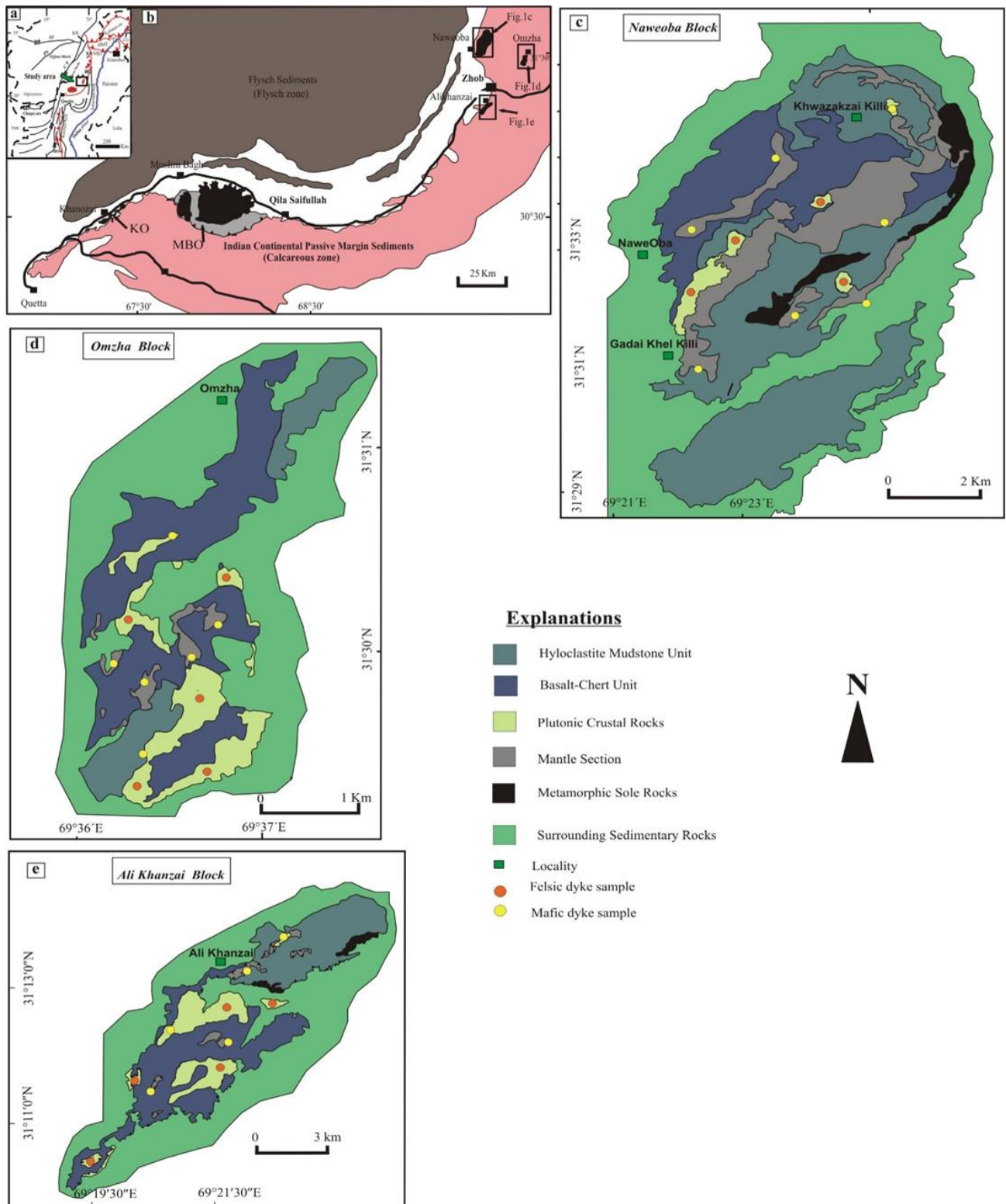


Figure 1. (a) Geotectonic map of the western and north-western boundary of the Indian Plate with Afghan Block showing the ophiolites occurrences (b) shows Khanozai, Muslim Bagh and Zhub Ophiolites and surrounding sedimentary rocks (c, d and e) Geological map of Naweoba, Omzha blocks and Ali Khanzai blocks of the Zhub ophiolite. BO; Bela Ophiolite, KO; Khanozai Ophiolite, MO; Muslim Bagh Ophiolite, ZO; Waziristan Ophiolite, ZO; Zhub Ophiolite, DO; Dargai Ophiolite, CO; Chilas Ophiolite, CF; Chaman Fault, PS; Penjwai Suture, HF; Herat Fault, KB; Karakorum Block; MMT; Main Mantle Thrust; MBT; Main Boundary Thrust (modified after Jones, 1961; Naeem et al, 2021)

Small light gray felsic dyke occurs in the gabbroic section the Omzha block which is intensely tectonized by faults and shear zones (Fig. 2c). The tectonic inclusions of the felsic and mafic dyke swarms are found in the serpentine mélanges which are derived from fragmented sections of ophiolite (Fig. 2d). In the Ali Khanzai block, parts of the plagiogranite body are highly altered and most of the samples show epidotization (Fig. 2e). Significant number of fresh and altered felsic dykes are present in the lower part of the gabbroic rocks near Naweoba Killi in the Naweoba block (Fig. 2f). The felsic rocks are in faulted contact with volcanic and volcanoclastic rocks and are in transitional contact with mafic rocks at several localities in the Zhub ophiolite. The mafic (dolerite) dykes are light gray to dark gray, fine to medium-grained with variable degrees of alteration. The mafic dykes range in thickness from a few centimeters to five meters and several hundred meters in length. The mafic dykes crosscut the mafic and ultramafic rocks of all three ophiolitic blocks. In the Ali Khanzai block these mafic dykes are not well-exposed and are mostly broken and sheared along with country rocks. The dykes do not show cross-cutting relationships with one another, but joints and fractures are very common. Massive dolerite dyke in Naweoba block intruded in ultramafic rocks (Fig. 3a). Dolerite dyke showing intruded contact with harzburgite in Omzha block of the Zhub ophiolite (Fig. 3b). The dykes in Naweoba block are intruded as massive bodies in gabbroic rocks (Fig. 3c). Hard and compact dolerite dykes intruded in gabbroic rock of the Naweoba block (Fig. 3d). The interaction of dolerite rocks remelted host rocks and formed chilled margin near Shiakhan Killi north of Ali Khanzai block of the Zhub ophiolite (Fig. 3e). Furthermore, the studied dykes are common in the peridotite and make sharp intrusive contacts with peridotite at some localities in the Ali Khanzai block (Fig. 3f). The dolerite dykes are altered and fragmented near Konnai Killi in the south of Omzha Block due to extensive tectonic activity and several concealed faults in the region (Fig. 3g). These dykes commonly exhibit usually intrusive contacts with host peridotite in the Naweoba block (Fig. 3h).

4. Petrography

4.1. Felsic Dykes

The Zhub ophiolite plagiogranite dykes are light grey to creamy white, fine to coarse-grained, and contain abundant quartz, microcline, orthoclase and plagioclase. In thin section the plagiogranite is extremely fractured and quartz is present as clusters that are surrounded by epidote crystals aggregates (Fig. 4a). The quartz grains are fresh and comprised on average 40% of the rock with (35%) plagioclase, with mafic (usually hornblende and pyroxene)

minerals being minor constituents (<10%) and K-feldspar (orthoclase) being a rare phase. A few samples of plagiogranite show large crystals of euhedral to subhedral plagioclase with quartz and minor amphibole (Fig. 4b). Accessory minerals are biotite, amphibole, calcite and opaque minerals. Chlorite, which is the alteration product of biotite and hornblende is present in Zhub ophiolite plagiogranite. Euhedral crystals of zircon with quartz and plagioclase are observed in a few thin sections of plagiogranite from the Naweoba block (Fig. 4c). Most plagioclase feldspar is partially altered. The epidote grains have a partially chloritized rim and sericite is observed as an alteration product of alkali feldspar. Plagiogranite shows massive, subhedral to anhedral, hypidiomorphic and inter-granular texture and anhedral to subhedral crystals of plagioclase with quartz (Fig. 4d). Phenocrysts of plagioclase, quartz, hornblende and pyroxene are surrounded by a fine groundmass composed of plagioclase, quartz, hornblende, pyroxene, potassium feldspar and accessory phases. The plagioclase mostly shows zoning, and pyroxene is partially altered to chlorite (Fig. 4e). Anhedral crystals of quartz have undulose extinction. Plagiogranite from the Ali Khanzai and Omzha blocks has quartz, plagioclase and deformed biotite with inter-grown muscovite (Fig. 4f).

4.2. Mafic Dykes

Dolerite dykes of the Zhub ophiolitic blocks are aphanitic, fine to medium-grained, allotriomorphic, intergranular and have sub-ophitic texture. The dolerite dykes are composed of plagioclase, clinopyroxene, hornblende, magnetite and quartz grains and are chloritized with quartz aggregates (Fig. 5a, b). Clinopyroxene and plagioclase are primary minerals while zeolites, quartz and calcite are secondary minerals. Dolerite rocks are granular and have interlocking contacts between plagioclase and pyroxene crystals (Fig. 5c, d). Plagioclase occurs as phenocrysts and is partially altered to sericite. Sub-ophitic plagioclase phenocrysts occur both as laths and larger anhedral to subhedral prisms (Fig. 5e, f). The plagioclase laths are partially to completely altered to epidote, sericite and calcite and penetrate the hornblende and pyroxene minerals (Fig. 5g, h). The hornblende is commonly altered to chlorite but is replaced by biotite in places. Clinopyroxene is augite which is partly to completely altered to amphibole and magnetite and forms a considerable part of groundmass, while in the rocks from the Naweoba it is present as phenocrysts. In few thin sections of the Ali Khanzai block the augite is anhedral and has faint zoning. The fine-grained quartz aggregates are found among the main minerals. Secondary minerals such as calcite, epidote, chlorite, amphibole and quartz suggest that the dykes have been subjected to metamorphism under greenschist facies

conditions. Tiny, rounded grains of iron oxides fill the interstices between primary minerals while calcite veins occupy fractures in the rock.

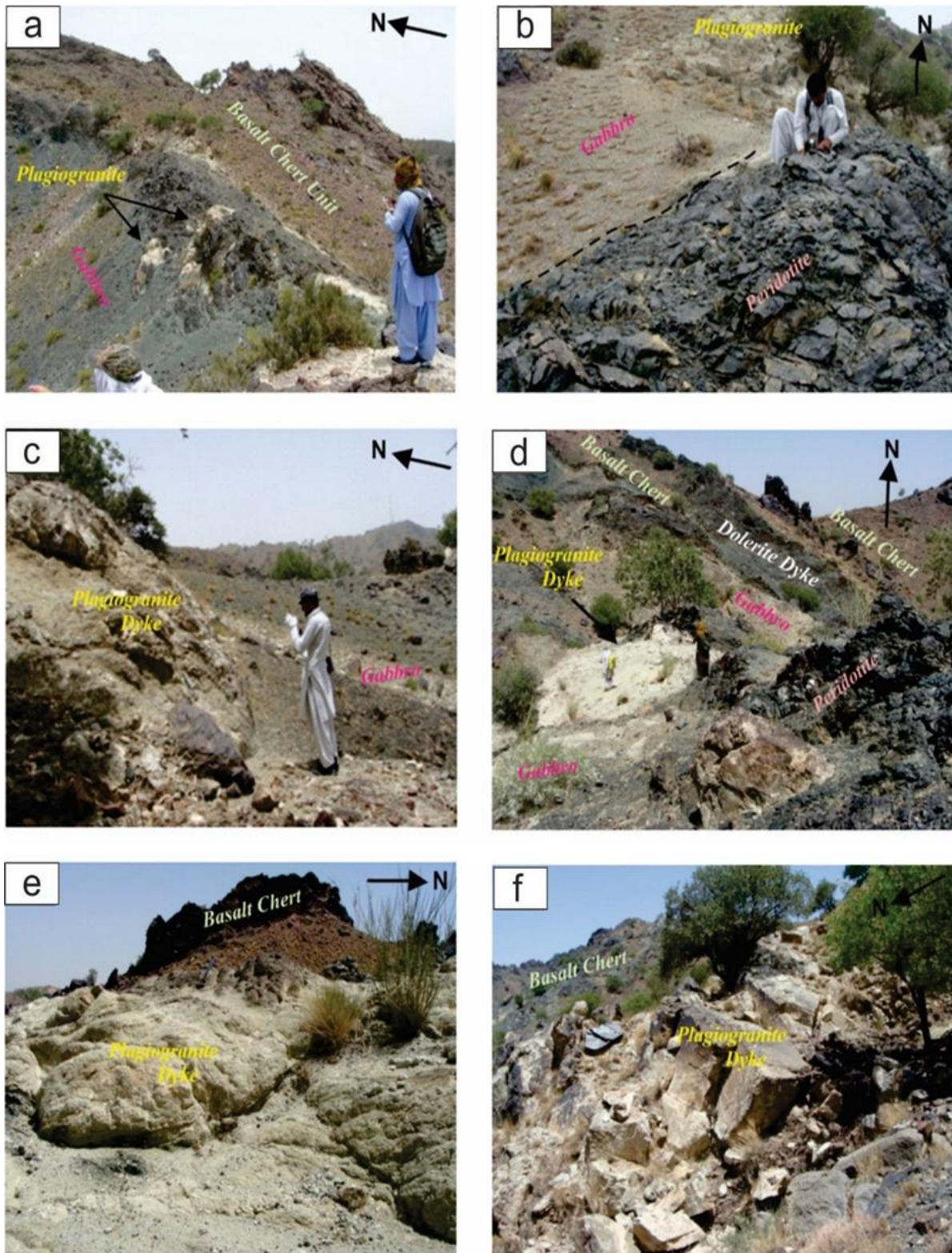


Figure 2. Field photographs showing, (a) a network of felsic veins (b) plagiogranite intruding gabbroic rock the intruded in the gabbroic rocks of the Zhub ophiolite (c) granitic rock intrusion in mafic rocks in the south of Yaseenzai Killi of the Omzha block (d) plagiogranite inclusions in serpentine mélanges (e) highly altered plagiogranite body in the Ali Khanzai block near Babar Killi (f) large intrusion of plagiogranite bodies in plutonic rocks near Naweoba Killi in Naweoba block

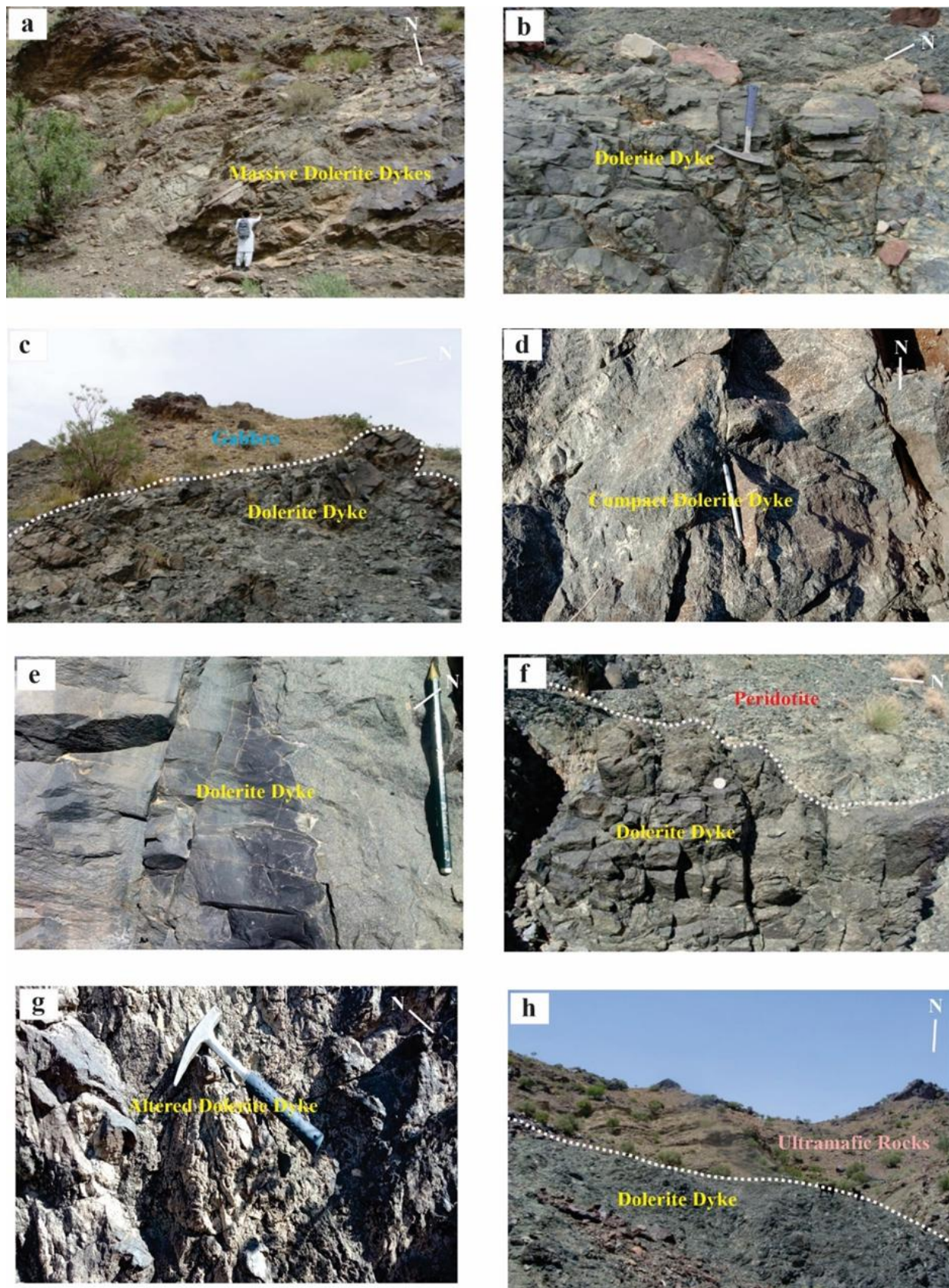


Figure 3. Field photographs showing, (a) dolerite dykes in ultramafic rocks in Naweoba block (b) in Omzha block (c) dolerite dykes (d) close-up view of dolerite dykes in gabbroic rocks in Naweoba block (e) chilled margin of dolerites near the Shiakhan Killi north of Ali Khanzai block (f) sharp intrusive contact of dolerite dykes with peridotite rocks in Ali Khanzai block (g) dolerite dykes near Konni Killi south of Omzha Block (h) dolerite rocks in dunite and harzburgite in Naweoba block

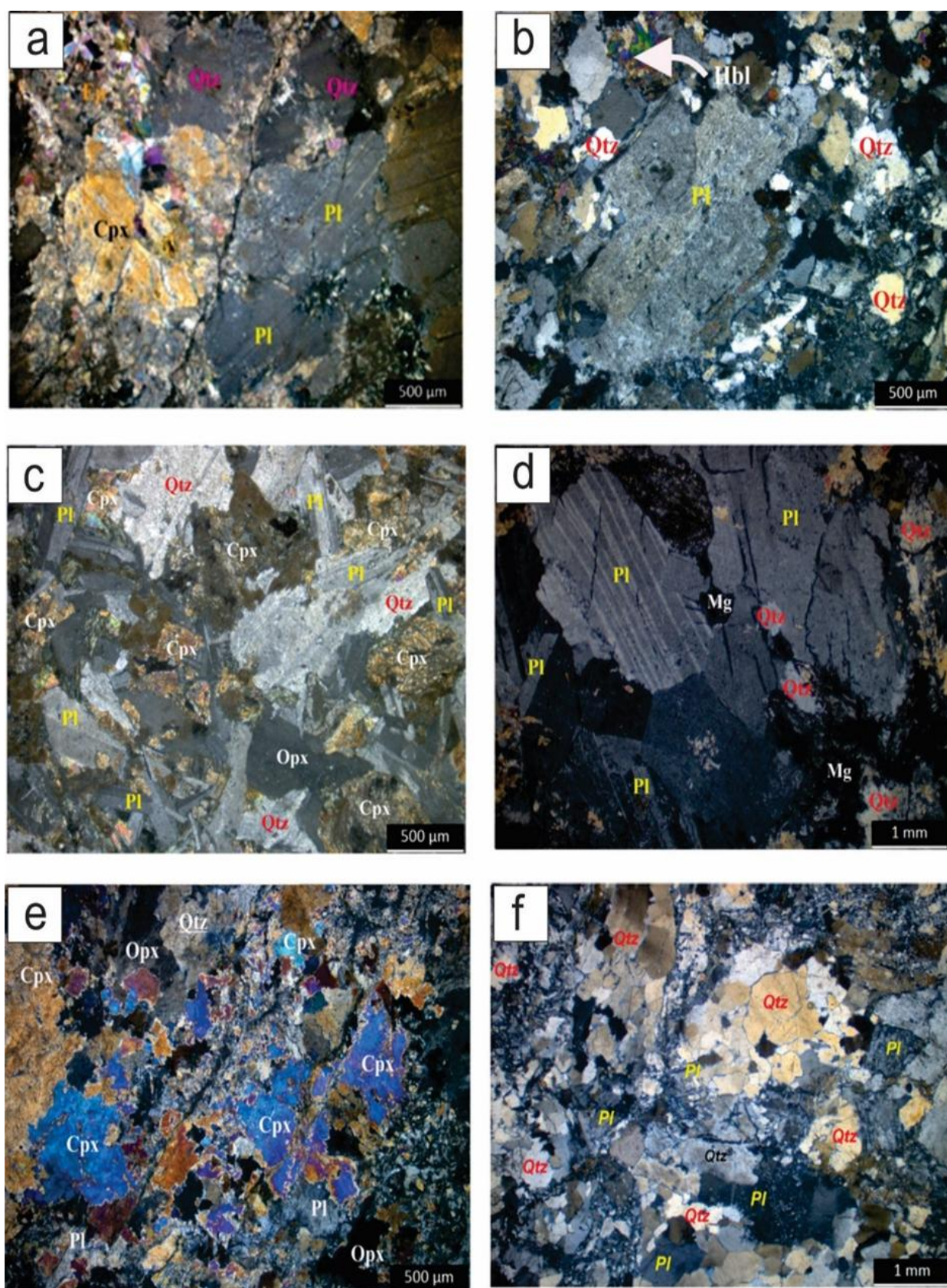


Figure 4. (a) plagiogranite showing subhedral quartz surrounded by epidote aggregates (XPL) (b) plagiogranite with large crystals of euhedral to subhedral plagioclase with quartz and minor amphibole (XPL) (c) plagiogranite containing plagioclase, quartz, minor clinopyroxene and euhedral crystals of zircon (XPL) (d) massive plagiogranite with subhedral to anhedral, hypidiomorphic and inter-granular texture and anhedral to subhedral crystals of plagioclase with quartz (XPL) (e) clinopyroxene in the plagiogranite partially altered to chlorite (XPL). (f) plagiogranite showing quartz, plagioclase and deformed biotite with inter-grown muscovite (XPL)

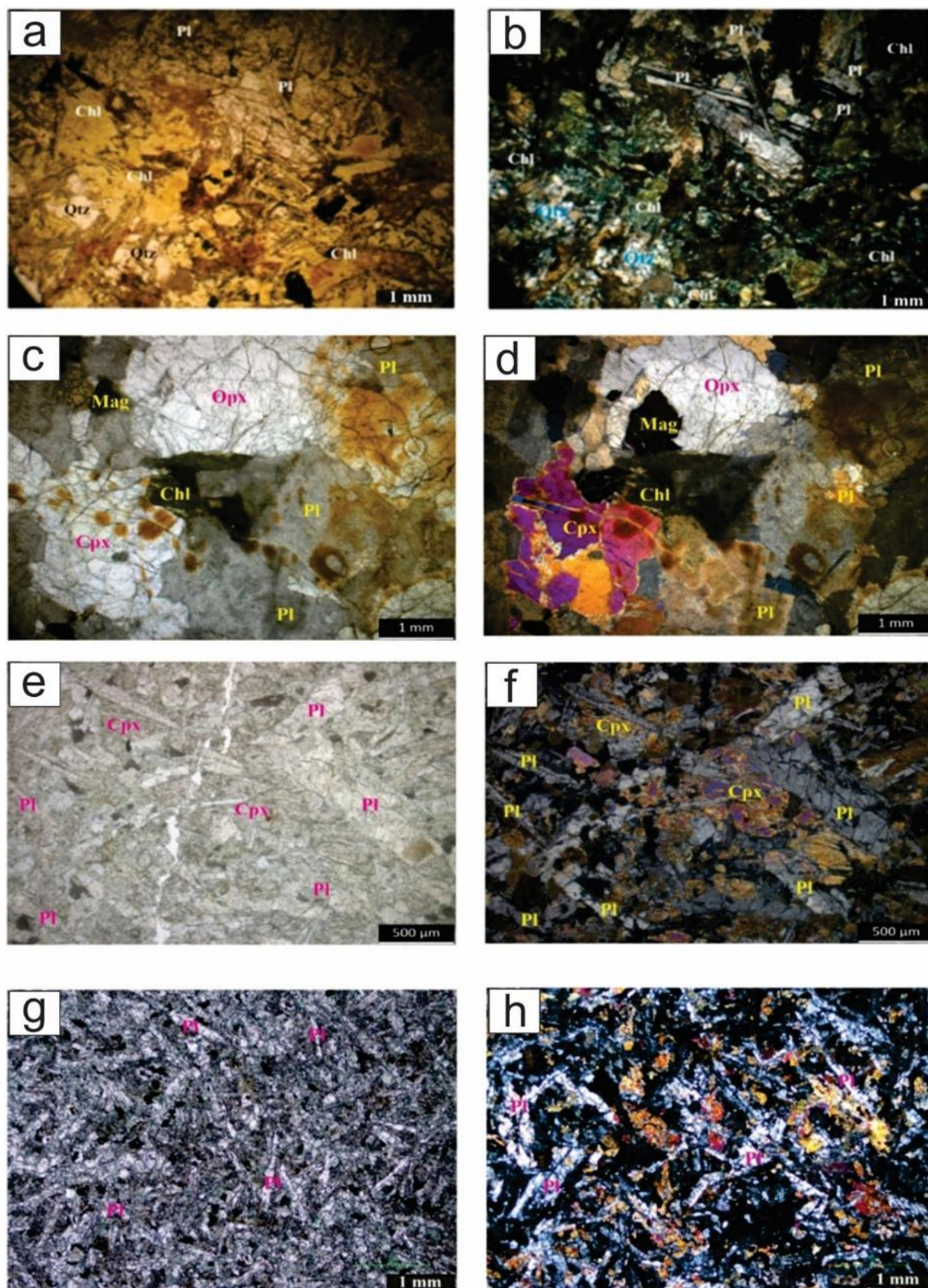


Figure 5. (a and b) Naweoba block dolerite dyke with sub ophitic texture and shows chloritization and fine quartz aggregates (a. PPL, b. XPL) (c and d) Omzha block dolerite dyke showing granular and interlocking contacts between plagioclase and pyroxene crystals (c. PPL, d. XPL). (e and f) Ali Khanzai block dolerite dyke with anhedral to subhedral plagioclase phenocrysts and augite phenocrysts with chloritization (e. PPL, f. XPL) (g and h) plagioclase laths penetrating pyroxene and hornblende (g. PPL, h. XPL)

5. Analytical Methods

Rock samples of both felsic and mafic dykes from the three ophiolitic blocks of the Zhub ophiolite were analyzed. Samples were powdered to 200 mesh after removing the weathered surfaces. Each powder sample was heated for two hours to 900°C in a porcelain crucible to obtain the loss on ignition. Inductively coupled plasma optical emission (ICP-OES) and inductively coupled plasma mass spectrometry (ICP-MS) were used to analyze the major, trace and rare earth elements in the School of Earth and Environmental Sciences, Cardiff University, Wales, UK.

In a platinum crucible 0.4 g of lithium metaborate flux was mixed with 0.1 g ignited sample. A few drops of wetting agents such as lithium iodide were added in each mixture for fusion by using the Claisse Flaxy automated fusion system. The mixture was then dissolved in 30 ml of de-ionized water and 20 ml of 10% HNO₃ by using the Milli-Q purification system. When the mixture had fully dissolved, and the solution was made up to 100 ml with 20 de-ionized water then 1 ml of 100 ppm Rh spike was added to the solution. At the end 20 ml of each solution was run on ICP-OES to determine the major element and some trace element abundances. To obtain the abundances of trace elements, 1 ml of each solution was added to 1 ml of In and Tl and 8 ml of 2% HNO₃ was run on the ICP-MS. The instruments used to analyze elements were, a JY von Horiba Ultima 2 ICP-OES and a thermos elemental X7 series ICP-MS at Cardiff University Wales, UK.

6. Results

Five mafic (dolerite) and four felsic (plagiogranite) dyke samples from Zhub ophiolites were analyzed for major, trace and rare earth element geochemistry. The major oxides from the mafic dykes of the Zhub ophiolite have the following range of compositions: MgO (1.7–5.7 wt.%), CaO (4.0–14.3 wt.%), TiO₂ (0.3–1.3 wt.%), Na₂O (0.4–6.0 wt.%), K₂O (0.02–1.3 wt.%), SiO₂ (47.6–56.7 wt.%), Al₂O₃ (12.8–15.2 wt.%), and Fe₂O₃ (10.7–12.5 wt.%). The range of trace elements are; Sc (8–43 ppm); V (11–351 ppm), Cr (3–39 ppm), Co (3–552 ppm), Ni (1–501 ppm), Cu (8–173 ppm), Zn (15–69 ppm), Sr (68–799 ppm), Y (16–31 ppm), Zr (29–77 ppm), and Ba (11–238 ppm). The major oxides from the felsic dykes of the Zhub ophiolite have the following compositional range: CaO (0.5–18.4 wt.%), TiO₂ (0.03–0.2 wt.%), alkalis (Na₂O + K₂O = 3.1–10.7 wt.%), MgO (0.1–1.3 wt.%), Al₂O₃ (10.1–18.2 wt.%), Fe₂O₃^t (0.2–1.4 wt.%), and SiO₂ contents (68.9–77.9 wt.%). The range of trace elements are; Sc (1–21 ppm), V (0–30 ppm), Cr (1–14 ppm); Co (1–5 ppm), Ni (2–13 ppm), Cu (2–4 ppm), Zn (2–26 ppm), Sr (59–163 ppm), Y (13–32 ppm), Zr (23–65 ppm), and Ba (8–43 ppm).

The felsic and mafic dyke samples were plotted on Zr and MgO Harker-type binary diagrams against other major and trace elements to determine fractionation trends of these rocks. On binary plots of the MgO versus other elements, the felsic and mafic dykes show some degree of clustering and scattering (Fig. 6 a, b). Major oxides and trace elements of felsic dykes such as Fe₂O₃, SiO₂, TiO₂, Sr, Nb, and Co versus MgO show clustering while Na₂O, Al₂O₃, CaO, Ni, Zr, and V versus MgO exhibit scattered patterns. Major oxides and trace elements of mafic dykes such as SiO₂, Na₂O, Al₂O₃, Co, and Ni versus MgO show clustering while CaO, TiO₂, Fe₂O₃, Zr, Nd, and Nb versus MgO exhibit scattered patterns. On binary plot of TiO₂ vs. Mg the dolerite dykes of the Zhub ophiolites with high MgO and low TiO₂ show small degrees of fractional crystallization. On the TiO₂ versus Mg plot for dolerite dykes TiO₂ increases during fractional crystallization and decreases when the degree of partial melting increases.

Binary plots of Zr versus other elements for the felsic and mafic dykes also show some degree of scattering (Fig. 7a, b). The ratio of TiO₂ and Zr on TiO₂ versus Zr plot of dolerite dykes increases during fractional crystallization and decreases when the degree of partial melting increases. On total alkali versus silica (TAS) diagram (Le Bas et al., 1986), two samples of dolerite dykes fall in the field of basaltic andesite, two in trachy-basalt and one in the basalt field while two samples of felsic dykes fall in the dacite field and two samples fall in rhyolite field (Fig. 8a). On an immobile trace element Th versus Co diagram (after Hastie et al. 2007) the dolerite rocks plot in the basalt to dacitic – rhyolitic field (Fig. 8b). The felsic rocks were plotted on K₂O vs SiO₂ a diagram and indicate that these rocks are plagiogranites and calc-alkaline in composition (Fig. 9a, b). The Y versus Nb diagram (Pearce et al., 1984), (Fig. 9c) classify these felsic rocks as volcanic arc granites (VAG) or ocean ridge granites (ORG). A volcanic arc setting is also confirmed by the Y versus Nb/Th plot (Jenner et al., 1991), (Fig. 9d). La-SiO₂ diagram (Brophy, 2009) suggests melting of a depleted source region for these felsic/mafic dyke rocks (Fig. 10). The dolerite dyke samples fall in basalt andesite and basalt field when plotted on Nb/Y versus Zr/Ti diagram of Pearce (1996), (Fig. 11a). On Zr versus P₂O₅ and Nb/Y versus Ti/Y diagrams (Winchester and Floyd, 1976; Pearce, 1982), (Fig. 11 b, c) the dolerite rock samples classify as N-MORB and arc rocks. Similarly, on Ti versus Zr (Pearce, 1981), Y versus Nb/Th (Jenner et al., 1991) and V versus Ti diagrams (Shervais, 1982), these mafic dyke rocks plot as N-MORB and IAT or BAB (Fig. 11d, e, f). The Na₂O vs K₂O diagram (Fig. 10g) confirms the sodic composition of rocks while the Ba versus Zr plot (Saunders and Tarney, 1991) further indicate their BABB and N-MORB type nature (Fig. 11h). Triangular MnO/TiO₂/P₂O₅ diagram

(Mullen 1983) conform the tholeiitic nature of these mafic rocks (Fig. 11i). On an N-MORB normalized plot (Sun and McDonough, 1989), both the plagiogranite felsic and dolerite mafic dykes have flat high field strength (HFS) element patterns parallel to N-MORB (Fig. 12a), while the large ion lithophile (LIL) elements are more enriched than N-MORB (Fig. 13a). On chondrite normalized diagrams (Fig. 12b and 13b), the REE patterns of these dykes are almost flat like those of N-MORB with slight enrichment in LREE and negative Eu anomalies. The enrichment of

LILEs may be due to either alteration or addition through adding a slab derived hydrous component to the melt source region, i.e. a depleted mantle wedge. However, the positive anomaly of Th and negative anomaly of Nb relative to other incompatible elements in the NMORB-normalized plots support the latter possibility (Wood, 1980). The flat pattern of both the LREEs and the HREEs of the dyke suggest derivation from a depleted mantle source.

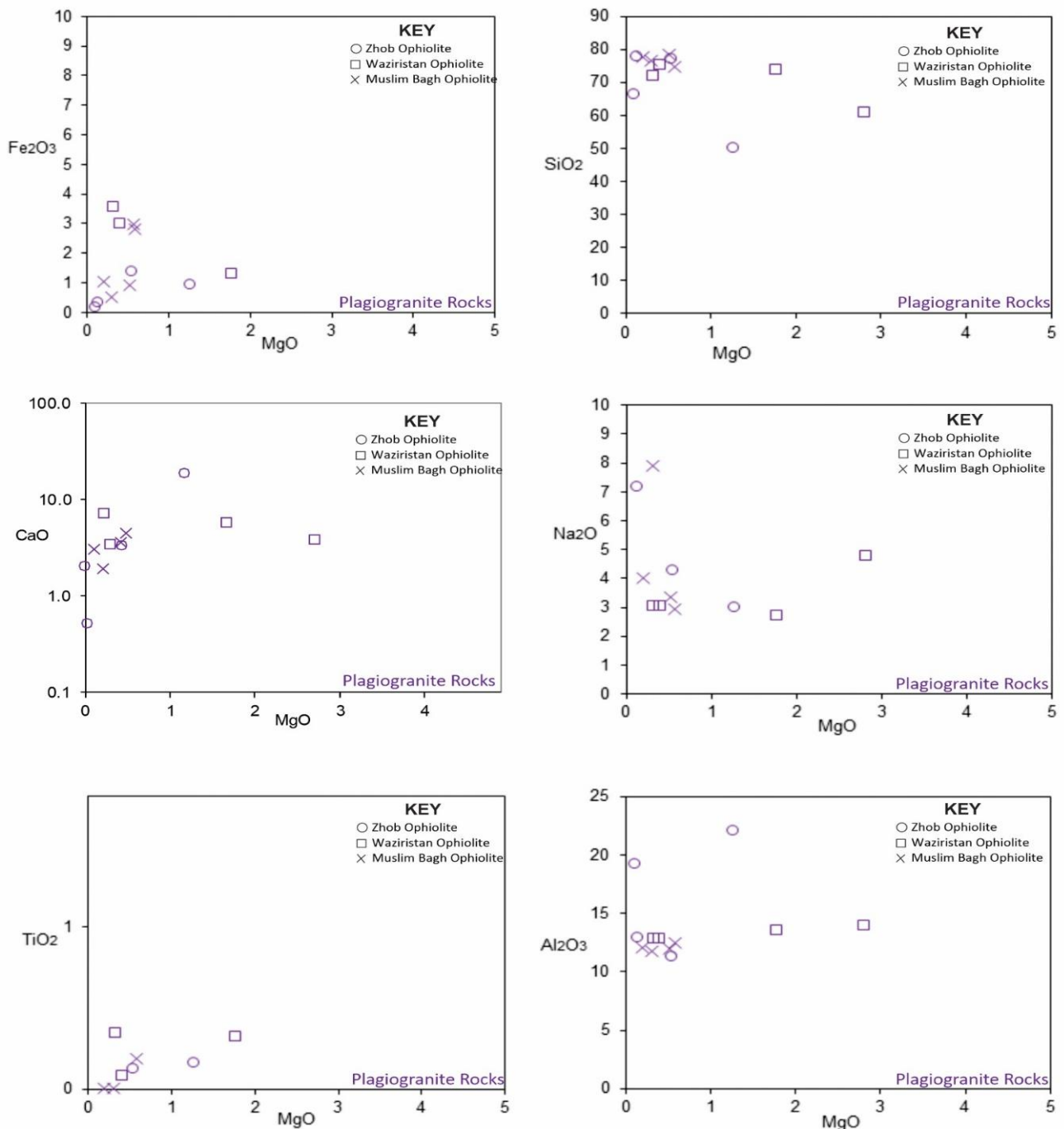


Figure 6a. Diagrams of MgO versus representative major and trace elements of the felsic dykes (blue). The analyses from the Muslim Bagh and Waziristan ophiolites are taken from (Kakar et al., 2014; Khan, 2000) respectively

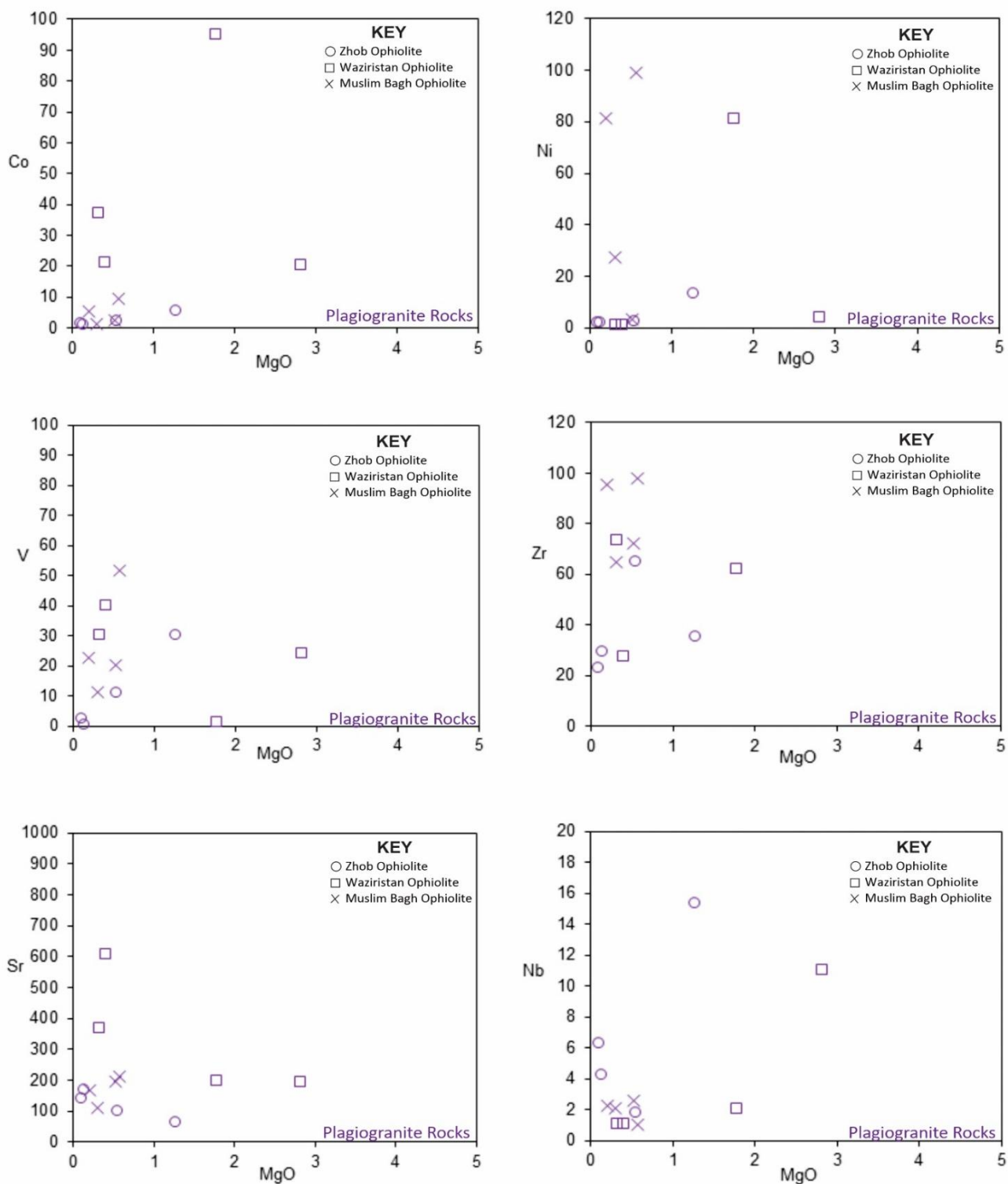


Figure 6a. Diagrams of MgO versus representative major and trace elements of the felsic dykes (blue). The analyses from the Muslim Bagh and Waziristan ophiolites are taken from (Kakar et al., 2014; Khan, 2000) respectively (Continued)

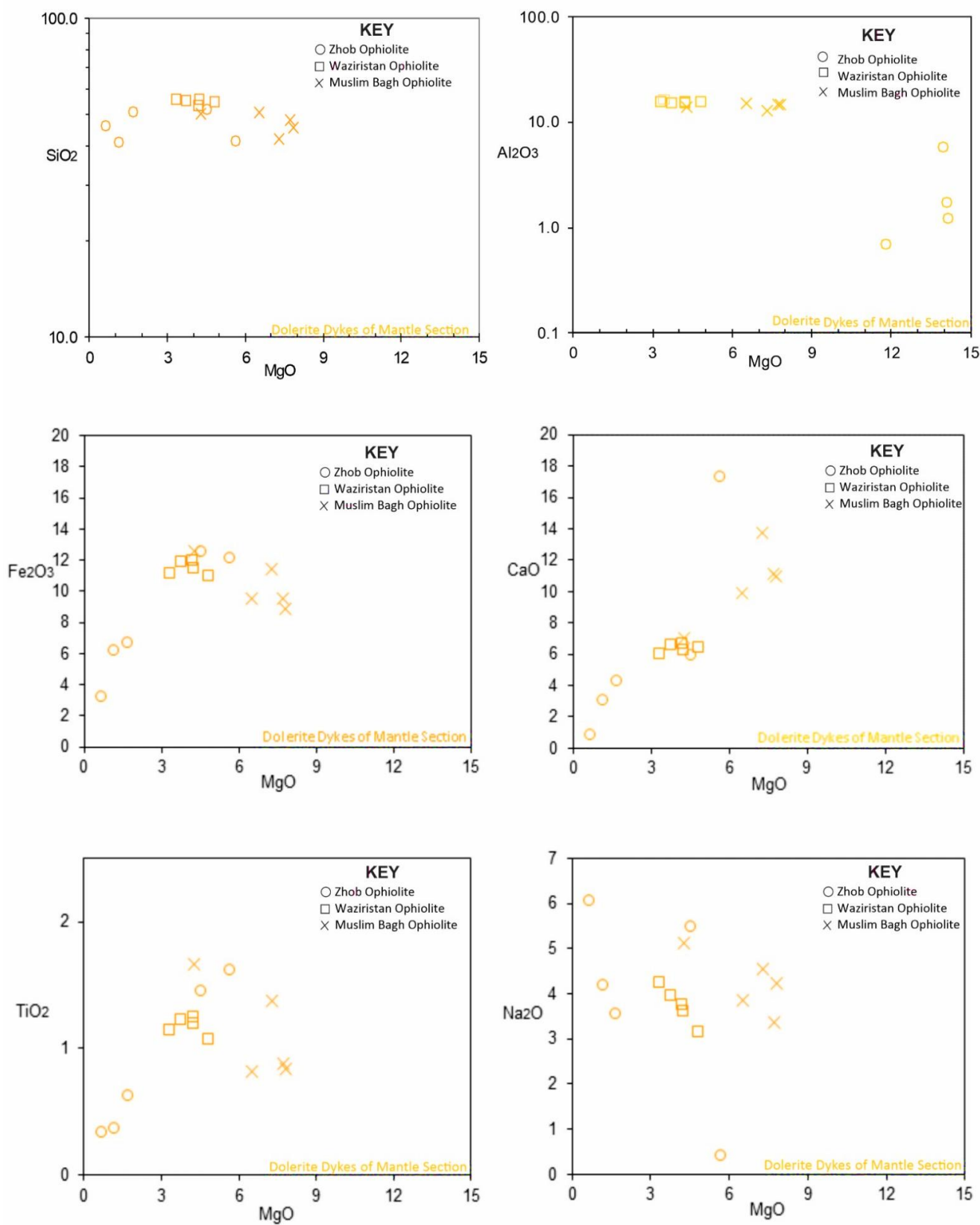


Figure 6b. Diagrams of MgO versus selected major and trace elements of the mafic dykes (yellow) of the Zhob ophiolite. The analyses from the Muslim Bagh and Waziristan ophiolites are taken from (Kakar et al., 2014; Khan, 2000) respectively

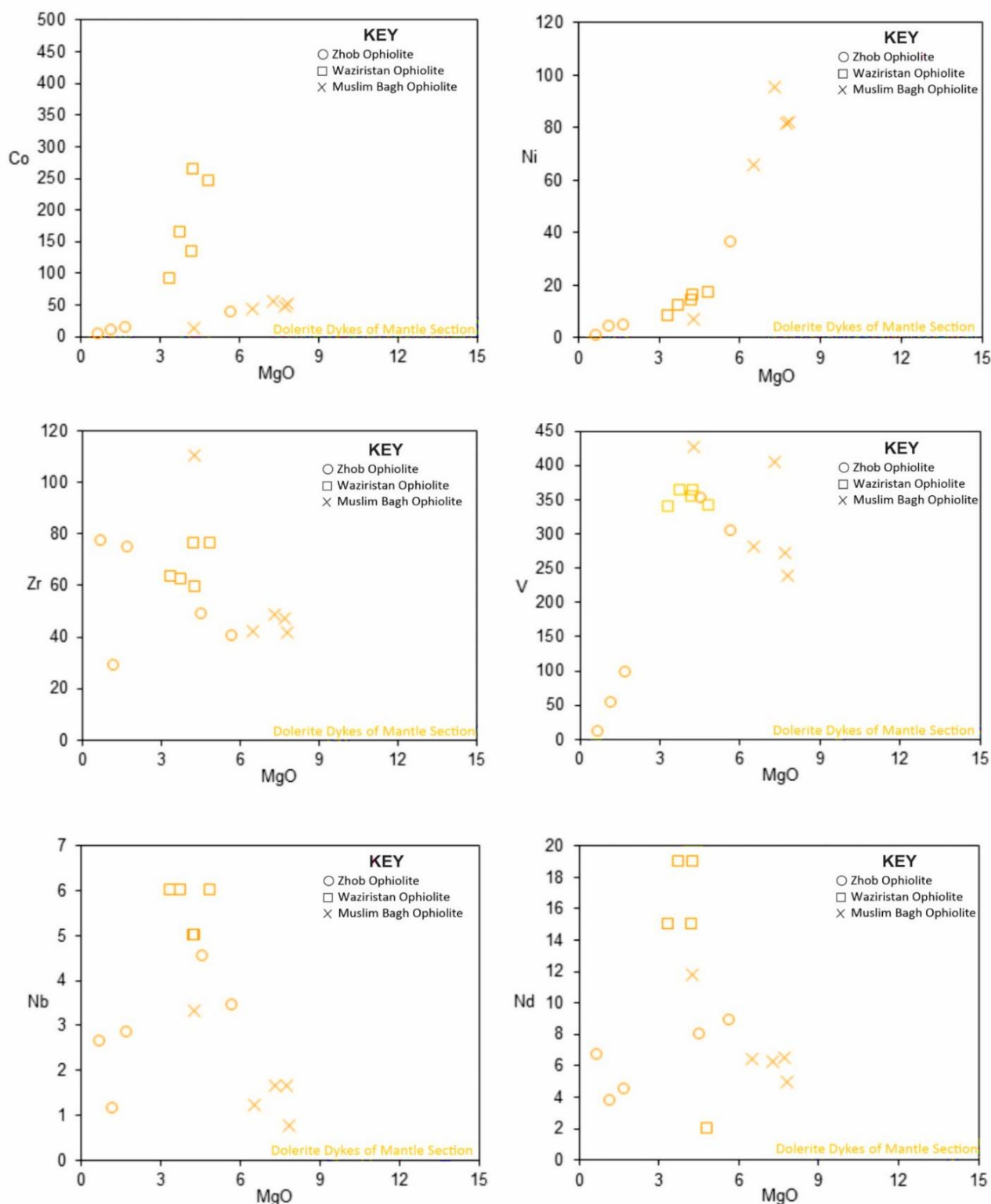


Figure 6b. Diagrams of MgO versus selected major and trace elements of the mafic dykes (yellow) of the Zhob ophiolite. The analyses from the Muslim Bagh and Waziristan ophiolites are taken from (Kakar et al., 2014; Khan, 2000) respectively (Continued)

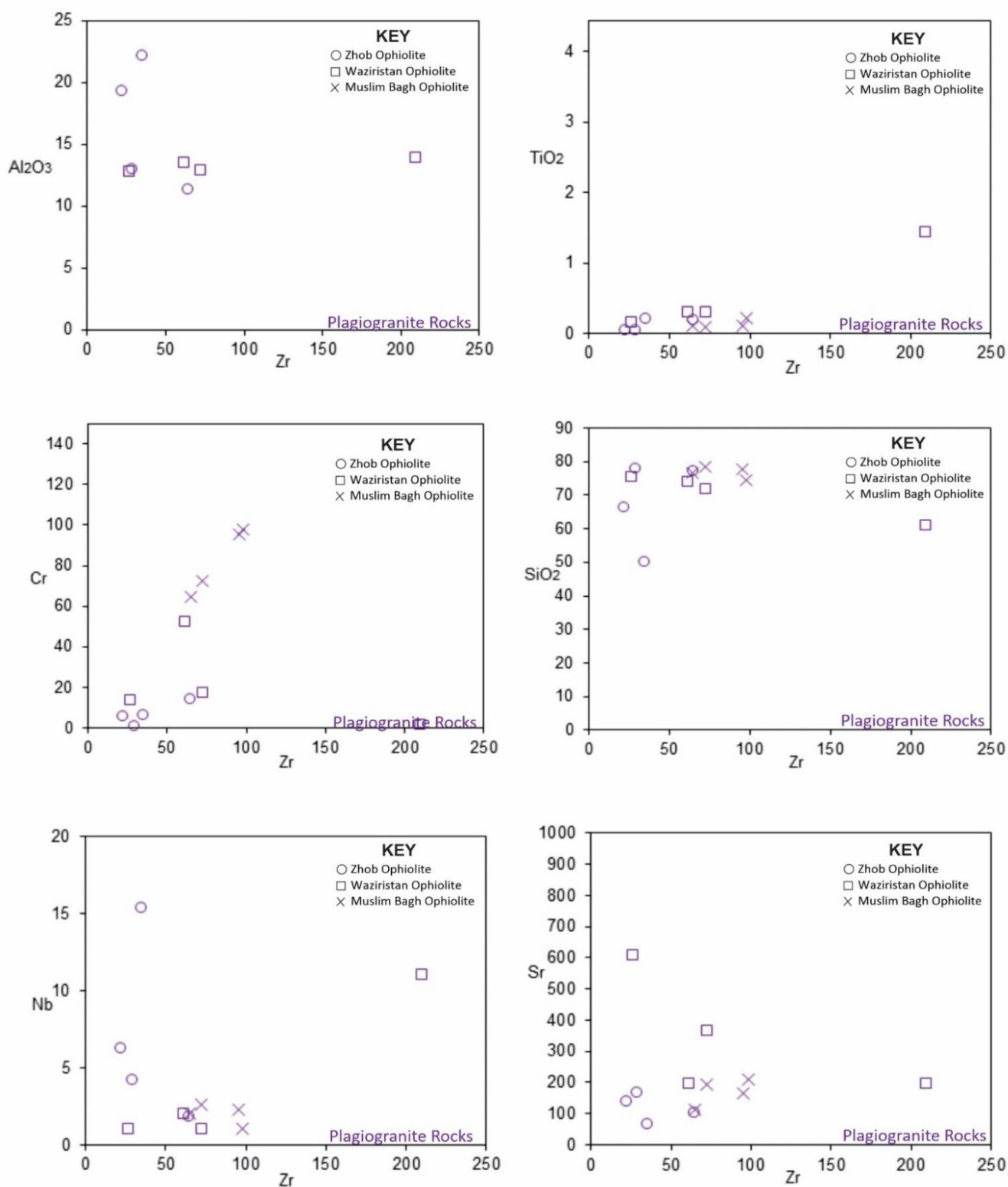


Figure 7a. Diagrams of Zr versus representative major and trace elements of the felsic dykes (blue). The analyses from the Muslim Bagh and Waziristan ophiolites are taken from Kakar et al. (2014) and Khan, (2000). respectively

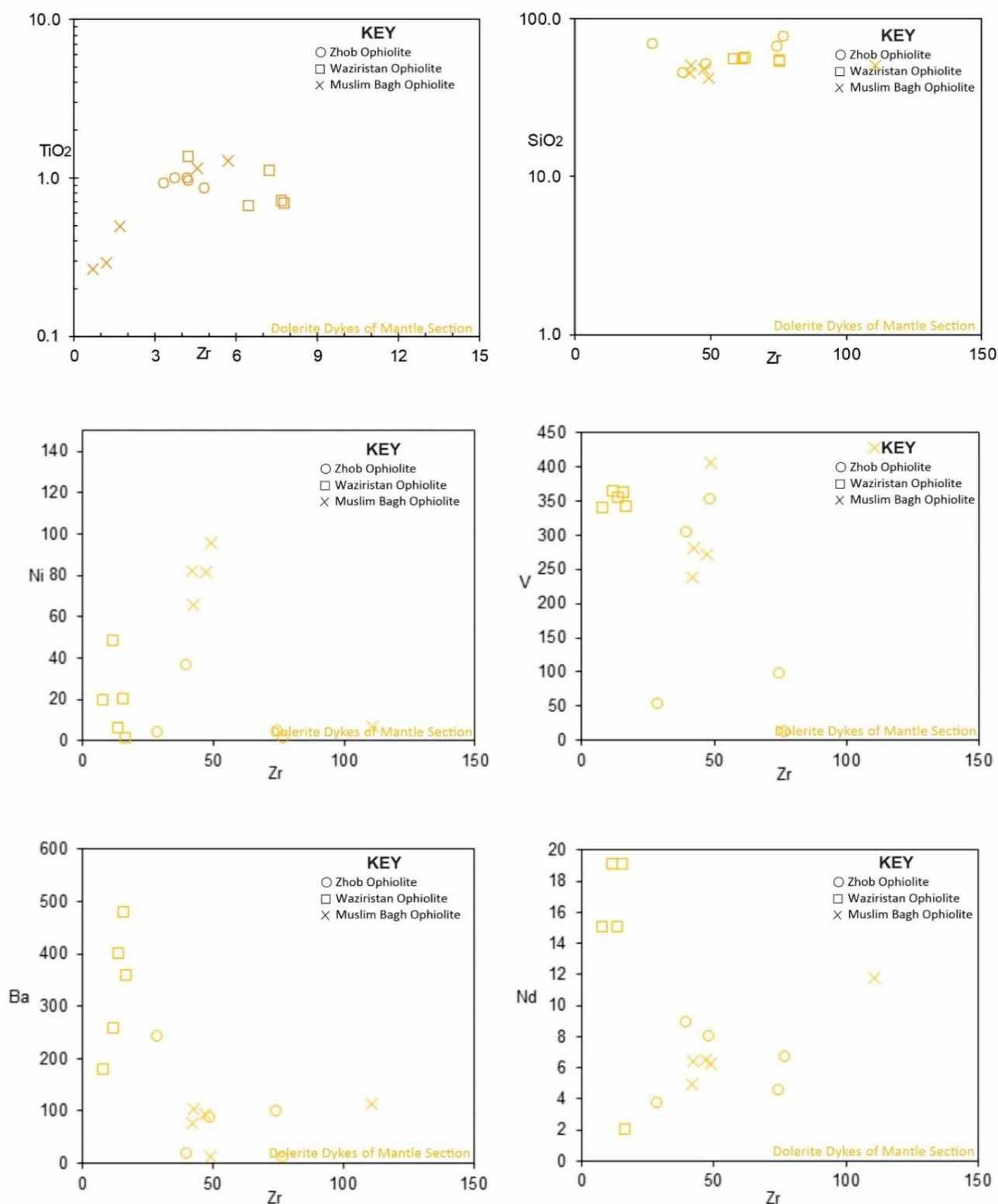


Figure 7b. Diagrams of Zr versus selected major and trace elements of the mafic dykes (orange) of the Zhob ophiolite. The analyses from the Muslim Bagh and Waziristan ophiolites are taken from Kakar et al. (2014) and Khan, (2000). respectively

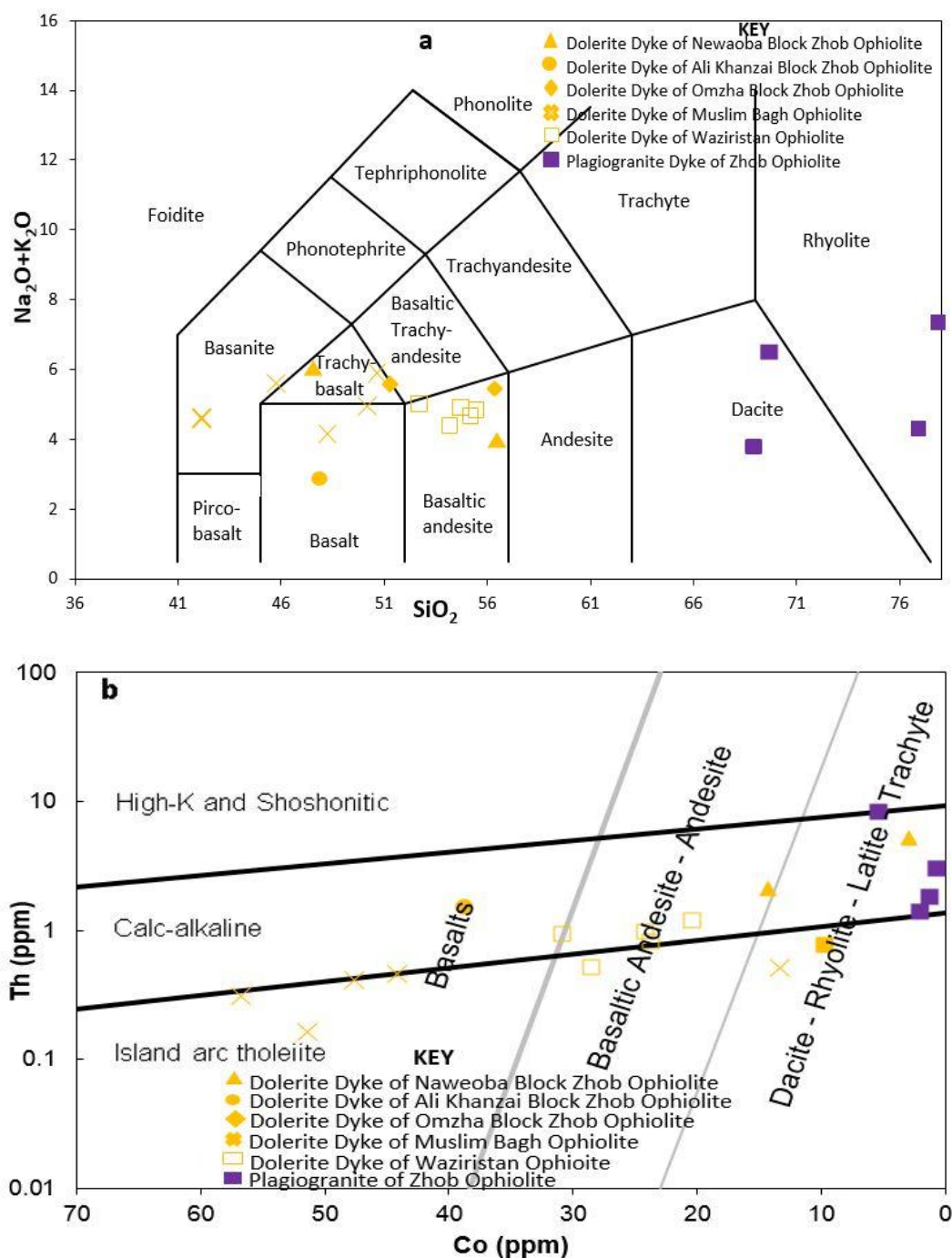


Figure 8. (a) Total alkali versus SiO₂ plot of the mafic dolerite dykes (yellow), (after Le Bas et al., 1986). (b) Classification of altered mafic dolerite dykes (yellow) of Zhob ophiolite using the Th–Co classification diagram (immobile trace elements) (after Hastie et al., 2007). The analyses from the Muslim Bagh and Waziristan ophiolites are taken from Kakar et al. (2014) and Khan, (2000), respectively

7. Discussion

Plagiogranites that contain more than 15 wt.% Al₂O₃ were likely generated in a continental setting whereas those containing less than 15 wt.% Al₂O₃ are considered to have been formed in an oceanic ridge setting (Arth, 1979; Pearce et al., 1984). The felsic dykes of the Zhob ophiolite contain less than 15 wt.% Al₂O₃ are oceanic plagiogranite. The Zhob plagiogranite dyke rocks are calc-alkaline in composition and fall below the line of partial melting of

depleted source that formed in volcanic arc setting. The dolerite dyke rocks of the Zhob ophiolite are basaltic to basalt-andesite in composition with low concentrations of TiO₂ and P₂O₅ and so are tholeiitic. The P₂O₅ versus Zr diagram and Ti/Y versus Nb/Y diagram further confirm the tholeiitic composition of these dolerite rocks. The dolerite dykes on Ti versus Zr, Nb/Th versus Y, V versus T, Ba versus Zr, TiO₂/MnO/P₂O₅ diagrams and the large ion lithophile (LIL) elements are more enriched than N-MORB

while high field strength (HFS) elements show a flat pattern parallel to N-MORB on an N-MORB normalized plot and suggest that these dykes are transitional between IAT and MORB. The enrichment of LIL elements over the high field strength (HFS) elements and depletion in Nb indicate an arc-related origin (Tankut et al., 1998; Robinson et al., 2008). This is explained by the addition of a hydrous slab derived component to a depleted mantle wedge (Thirlwall et al., 1996). The crustal part of the Zhob ophiolite has a less-well developed gabbroic section with a relatively thick ultramafic-mafic cumulate section and geochemical signatures that indicate an island arc or supra-subduction setting (Naeem et al., 2022). The REE patterns of both felsic and mafic dykes are almost flat like those of N-MORB with slight enrichment in LREE and negative Eu anomalies on chondrite diagrams. The normalized REE and trace diagrams further indicate the transitional character of these felsic and mafic dykes between N-MORB and IAT and the enrichment of LIL element and depletion of Nb suggest supra subduction zone tectonic setting.

7.1. Petrogenesis

The bulk chemical compositions of the plagiogranites are similar to granite and rhyolite but plagiogranite contains $K_2O < 1\%$ while granite and rhyolite contain $K_2O > 3\%$. The felsic dyke rocks of the Zhob ophiolite with low TiO_2 , MgO and K_2O concentrations (< 1 wt.%) and high SiO_2 , Al_2O_3 and Na_2O are considered a key characteristic of oceanic plagiogranites that have been derived by partial melting, as opposed to oceanic plagiogranites derived through fractional crystallization that display higher TiO_2 contents (> 1 wt.%; Koepke et al., 2004, 2007).

Oceanic plagiogranite can be formed by fractional crystallization of sub-alkaline tholeiitic magma (Cox et al., 2019; Grimes et al., 2011) or partial melting of crustal rocks under hydrous conditions (Barker, 1979) or by liquid immiscibility or metasomatism (Dixon and Rutherford, 1979). On binary plots the major oxides and trace elements of felsic dykes such as Fe_2O_3 , SiO_2 , TiO_2 , Sr, Nb, and Co versus MgO show clustering while Na_2O , Al_2O_3 , CaO, Ni, Zr, and V versus MgO exhibit scattered patterns which indicate the fractional crystallization process (Fig. 6a, 7a). The plagiogranites of the Zhob ophiolite show their own distinct field (Fig. 6a, 7a) which indicates that they are not related to the other units by simple fractional crystallization processes. The Zhob ophiolite sequence is mostly mafic, ultramafic and felsic rocks with the absence of intermediate composition rocks, which indicate the fractional

crystallization process for the origin of the plagiogranite by a basic parental melt. Moreover, the SiO_2 range of the plagiogranites would suggest that fractional crystallization did not play a significant role in their petrogenesis. On chondrite normalized diagrams (Fig. 12b), the enrichment of La, Ce, Pr and concave-upwards patterns displayed by the plagiogranites support a role for amphibole during their petrogenesis, due to amphiboles preference for MREE over LREE and HREE (Davidson 2012). The enrichment of La, Ce and Pr does not indicate whether amphibole was crystallizing from a parental magma or acting as a residual phase during the fusion of a mafic protolith. An origin by silicate-liquid immiscibility (Dixon and Rutherford, 1979) is unlikely for the Zhob ophiolite plagiogranites. This is evidenced by the absence of the associated immiscible Fe-rich liquid (as Fe-rich mafic units) from the Zhob ophiolite. The Zhob plagiogranite dykes with high SiO_2 and low TiO_2 suggest that they were derived by partial melting of gabbroic rocks in the crustal sequence. The Brophy (2009) model on the behavior of REEs and SiO_2 was used to determine the petrogenesis of felsic rock of the Zhob ophiolite (Fig. 10). It is estimated that almost 70% felsic rocks within ophiolite complexes were generated by partial melting of depleted basalts or gabbros (Furnes and Delik, 2017). Based on geochemical characteristics and petrogenetic models, the Zhob plagiogranite dykes were formed as a result of high degrees of partial melting in the presence of water from subduction.

The mafic dykes of the Zhob ophiolite with high contents of LILEs and the flat pattern of the HFSEs and REEs, with no depletion in the LREEs are indicative of an IAT signature (Figure 12a, 13a). The enrichment of LILEs may be due to either alteration or addition of a slab derived hydrous component to the melt source region, i.e. a depleted mantle wedge. However, the positive anomaly of Th and negative anomaly of Nb relative to other incompatible elements in the NMORB-normalized plots support the latter possibility (e.g. Wood, 1980; Hofmann, 1997). The flat pattern of both the LREEs and the HREEs (with the exception of elements La and Ce) of the dolerite dyke suggest derivation from a depleted mantle source. The mafic rocks of the Zhob ophiolite (basalt and gabbro) have very low contents of La and the plagiogranite and diorite samples plot below the line of partial melting of a highly depleted source with no indication of derivation by fractional crystallization (Fig. 10). Hence, both felsic and mafic dyke rocks of the Zhob ophiolite are likely derived from partial melting of a depleted source.

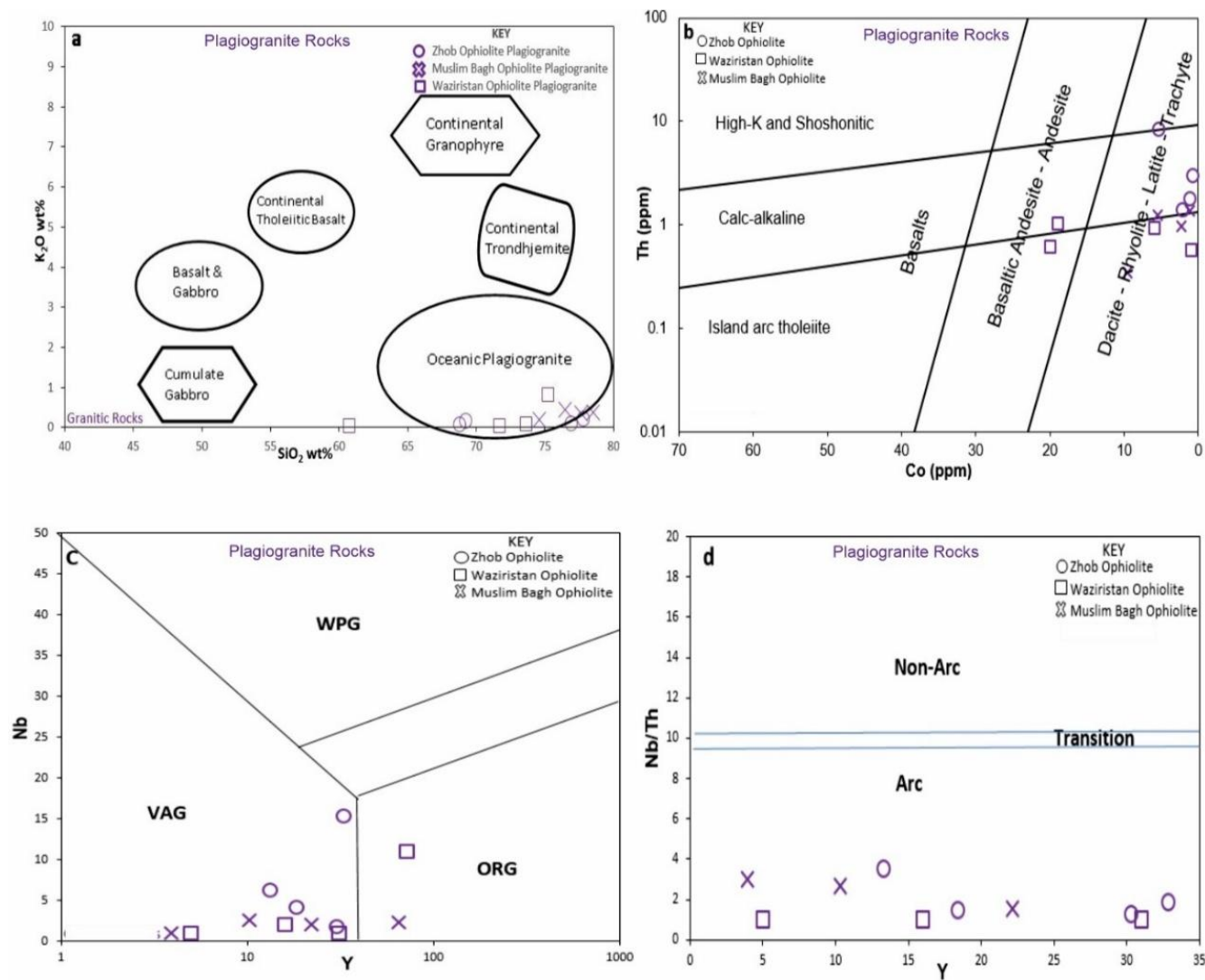


Figure 9. (a) Tectonic discrimination plots of the Zhob ophiolite granite SiO₂ versus K₂O plot (after Coleman and Peterman, 1985) (b) Co versus Th classification of altered granite using immobile trace elements (after Hastie et al., 2007) (c) Nb versus Y plot diagram (Pearce et al., 1984) (d) Nb/Y versus Y tectonic discrimination diagram (after Jenner et al., 1991). The analyses from the Muslim Bagh and Waziristan ophiolites are taken from Kakar et al. (2014) and Khan, (2000), respectively

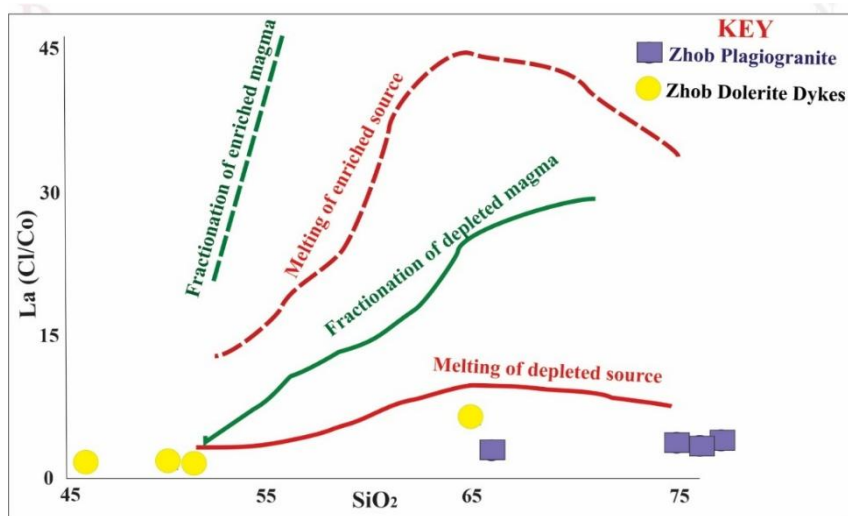


Figure 10. Felsic rocks and diorite dykes of the Zhob ophiolite are shown on La-SiO₂ diagram which is used to help determine the partial melting and fractional crystallization trend (Modified after Brophy, 2009)

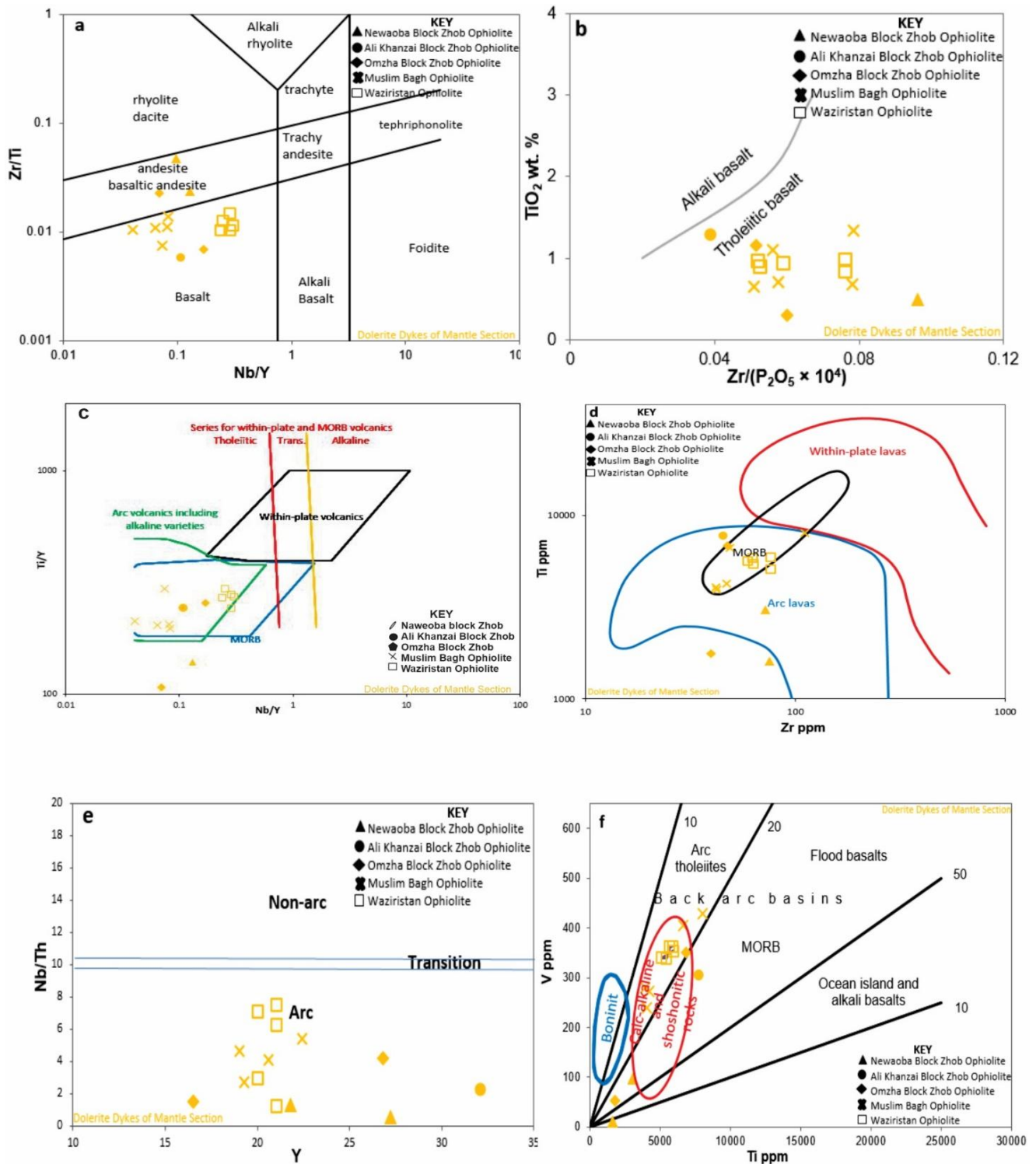


Figure 11. (a) Tectonic discrimination diagram of mafic dolerite dykes (yellow) on Zr/Ti versus Nb/Y (after Pearce, 1996) (b) Zr/P₂O₅ versus TiO₂ diagram (after Winchester and Floyd, 1976) (c) Nb/Y versus Ti/Y diagram (after Pearce, 1982) (d) Zr versus Ti diagram (after Pearce et al., 1981) (e) Nb/Y versus Y tectonic discrimination diagram (after Jenner et al., 1991) (f) Ti versus V diagram (after Dilek et al., 2011) (g) Na₂O versus K₂O diagram (after Middlemost, 1975) (h) MnO/TiO₂/P₂O₅ triangular diagram (after Mullen, 1983) (i) Ba versus Zr tectonomagmatic discrimination diagram (after Saunders and Tarney, 1991). The analyses of the Muslim Bagh and Waziristan ophiolites are taken from Kakar et al. (2014) and Khan, (2000), respectively

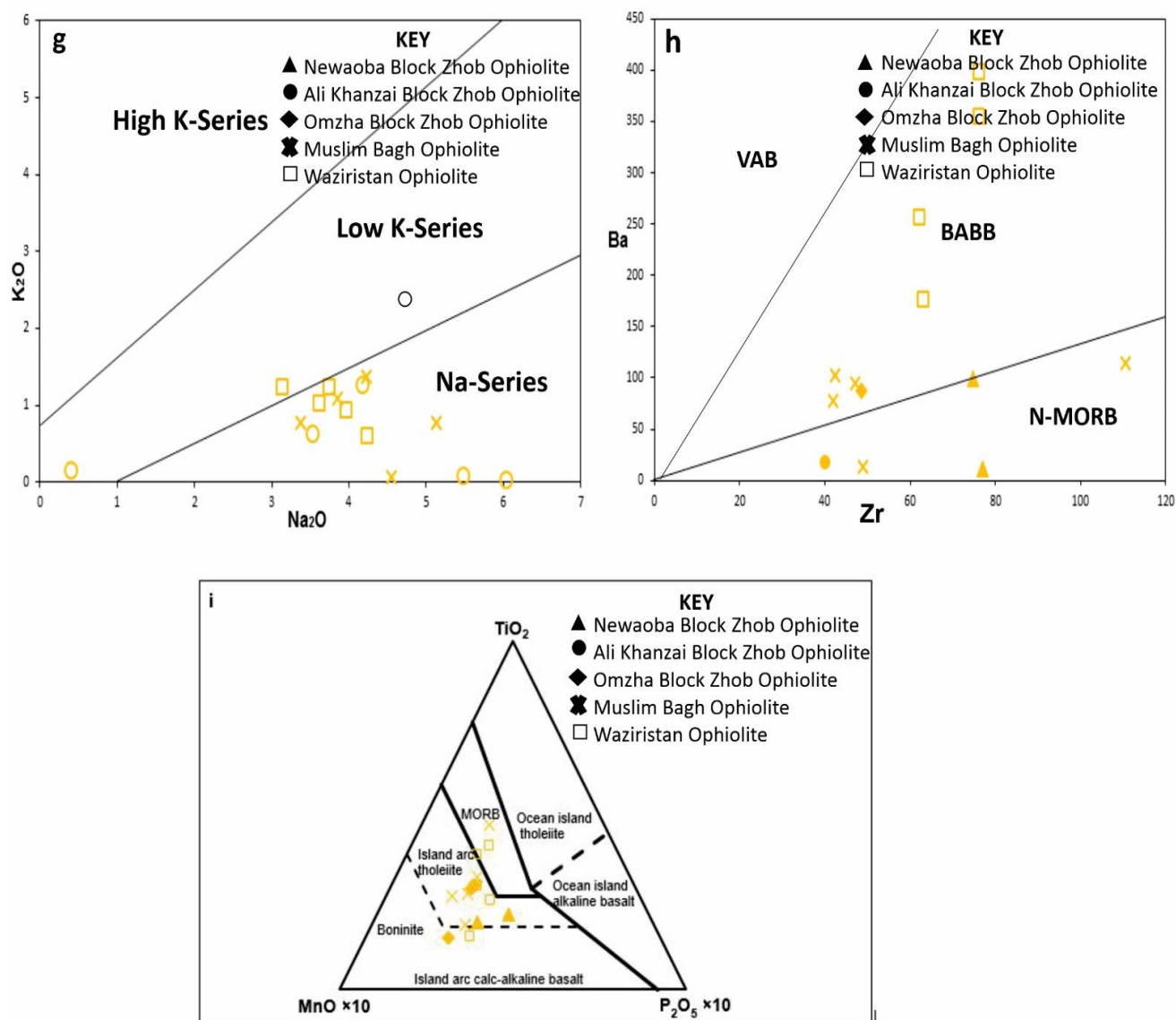


Figure 11. (a) Tectonic discrimination diagram of mafic dolerite dykes (yellow) on Zr/Ti versus Nb/Y (after Pearce, 1996) (b) Zr/P₂O₅ versus TiO₂ diagram (after Winchester and Floyd, 1976) (c) Nb/Y versus Ti/Y diagram (after Pearce, 1982) (d) Zr versus Ti diagram (after Pearce et al., 1981) (e) Nb/Y versus Y tectonic discrimination diagram (after Jenner et al., 1991) (f) Ti versus V diagram (after Dilek et al., 2011) (g) Na₂O versus K₂O diagram (after Middlemost, 1975) (h) MnO/TiO₂/P₂O₅ triangular diagram (after Mullen, 1983) (i) Ba versus Zr tectonomagmatic discrimination diagram (after Saunders and Tarney, 1991). The analyses of the Muslim Bagh and Waziristan ophiolites are taken from Kakar et al. (2014) and Khan, (2000), respectively (Continued)

7.2. Tectonic Setting

The Zhub, Muslim Bagh and Waziristan ophiolites plagiogranite dykes (Khan, 2000; Kakar et al., 2014) have K₂O and SiO₂ relationships, which suggest that these rocks were formed in oceanic tectonic setting. The Muslim Bagh Ophiolite formed $\sim 80.2 \pm 1.5$ Ma ago (Kakar et al., 2012) in a supra-subduction zone tectonic setting related to the west–northwest dipping subduction (Gnos et al., 1997) of a narrow branch of the Neo-Tethys Ocean (Mahmood et al., 1995; Kakar et al., 2014). Various plots based on LIL elements and HFS elements, e.g., Fig. 8c and d, suggest

that the plagiogranite dykes of the Zhub, Muslim Bagh and Waziristan ophiolites are transitional between volcanic arc granite (VAG) and oceanic ridges granite (ORG). The Nb content of volcanic arc granite (VAG) is less than 15 ppm while in plate granite (WPG) it is more than 15 ppm. The N-MORB normalized pattern of the Zhub plagiogranite shows LREE enrichment relative to HREE with very slight negative Nb and Ta anomalies and a marked depletion in Ti with a positive Th anomaly (Fig. 12a), which indicate that these rocks were generated in N-MORB and island arc settings and are supportive of a supra-subduction zone environment. Volcanic arc plagiogranites are chemically

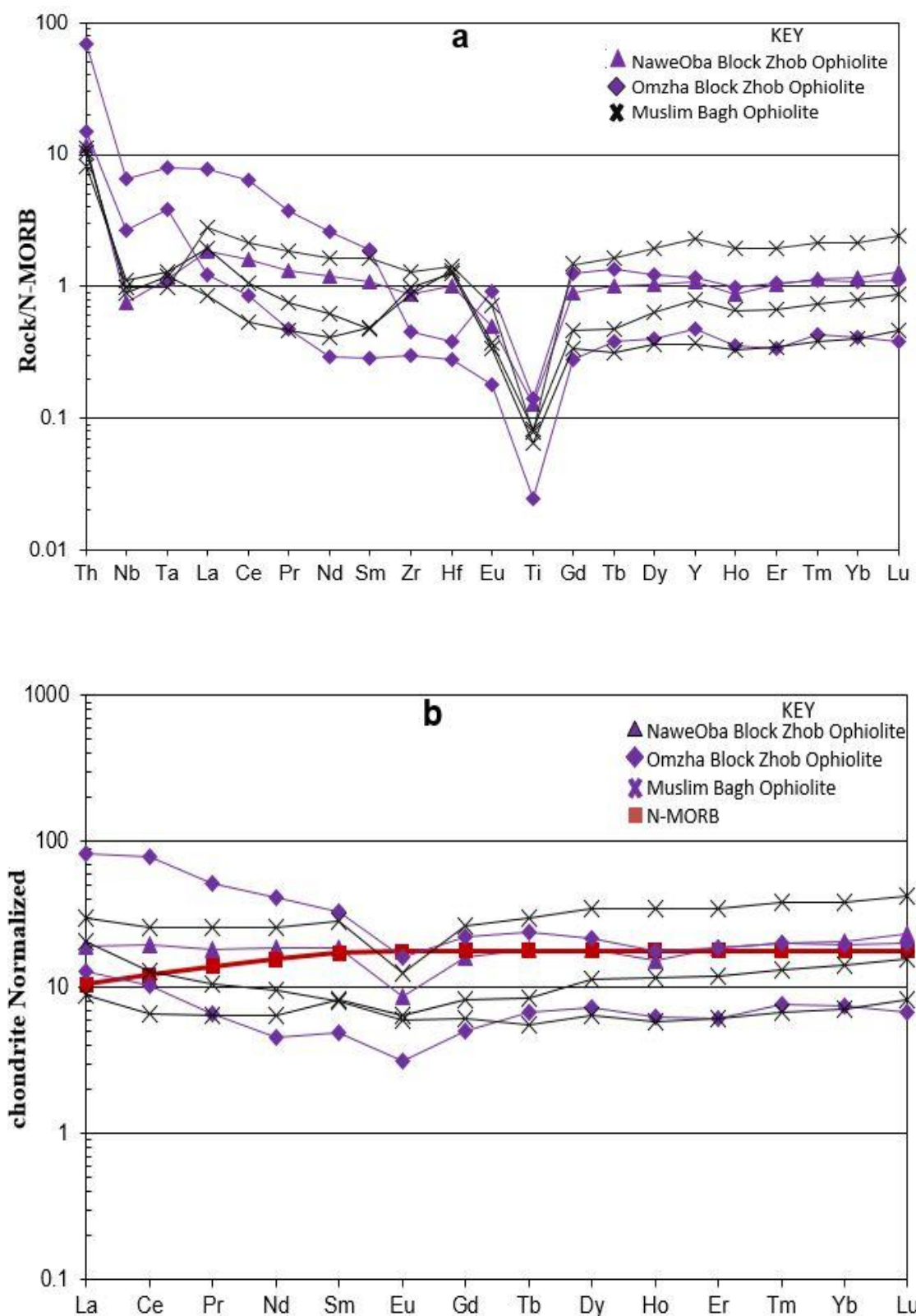


Figure 12. (a) Multi-element N-MORB normalized diagram of the felsic granite dykes (blue) of the Zhub ophiolite (b) chondrite normalized REE diagrams of the felsic granite dykes (blue) of the Zhub ophiolite (after Sun and McDonough, 1989). The analyses from the Muslim Bagh ophiolite are taken from Kakar et al., (2014)

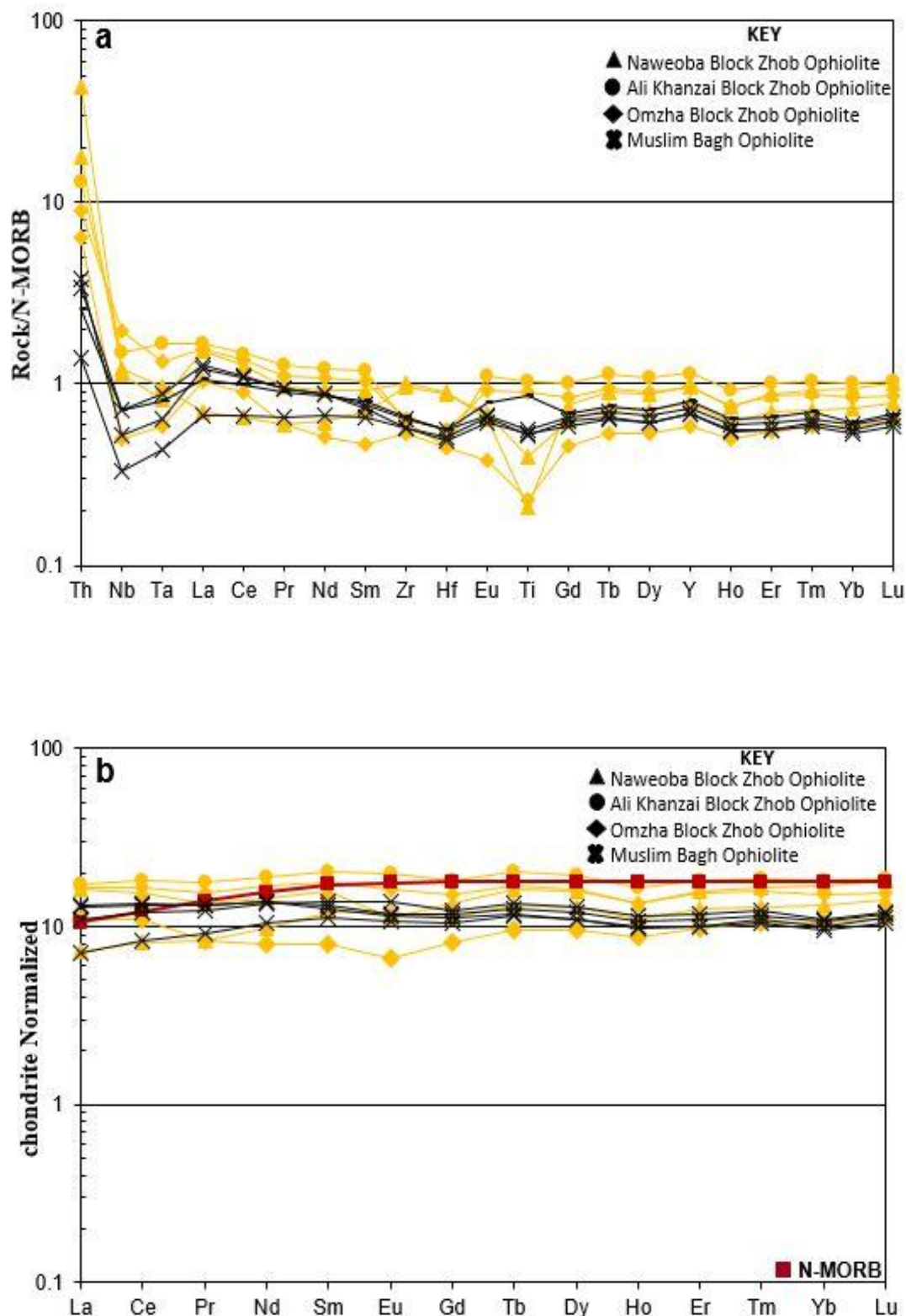


Figure 13. (a) Multi-element N-MORB normalized diagram of the mafic dolerite dykes (yellow) of the Zhub ophiolite (b) chondrite normalized REE diagrams of the mafic dolerite dykes (yellow) of the Zhub ophiolite (after Sun and McDonough, 1989). The analyses from the Muslim Bagh ophiolite are taken from Kakar et al., (2014)

Table 1. Major oxides (wt %), trace and REE elements (ppm) of the doleritic and plagiogranite dykes of the Zhub ophiolite

Sample No	NB 08	NB 20	AK 30	OMZ 03	OMZ 04	NB 45	OMZ 06	OMZ 43	OMZ 49
Rock Type	Dolerite	Dolerite	Dolerite	Dolerite	Dolerite	Plagiogranite	Plagiogranite	Plagiogranite	Plagiogranite
SiO ₂	56.69	47.61	47.93	51.31	56.70	76.94	69.29	77.85	68.85
TiO ₂	0.50	0.27	1.29	1.16	0.29	0.16	0.03	0.04	0.18
Al ₂ O ₃	14.12	12.84	13.99	15.20	14.20	11.29	18.23	12.92	10.07
Fe ₂ O ₃	10.68	11.19	12.06	12.47	11.12	1.35	0.16	0.31	0.92
MnO	0.13	0.05	0.20	0.19	0.12	0.02	0.01	0.01	0.02
MgO	1.71	4.68	5.68	4.56	1.19	0.55	0.11	0.14	1.28
CaO	4.22	9.79	14.28	5.92	3.99	3.26	2.01	0.51	11.41
Na ₂ O	3.53	6.04	0.41	5.48	4.18	4.25	10.42	7.15	2.99
K ₂ O	0.62	0.02	0.16	0.08	1.27	0.07	0.14	0.19	0.05
P ₂ O ₅	0.08	0.05	0.10	0.09	0.05	0.02	0.05	0.06	0.12
Cr ₂ O ₃	0.00	0.00	0.01	0.00	0.00	0.00	0.00	0.00	0.00
LOI	6.55	6.09	2.72	1.86	6.20	0.13	0.40	0.26	4.19
Total	98.92	98.61	98.84	98.33	99.31	98.04	98.84	99.45	100.08
Sc	20.5	8.1	42.9	31.1	19.6	8.7	3.0	1.2	21.4
V	97.0	11.0	303.9	351.4	52.4	11.1	2.4	0.3	30.2
Cr	6.5	4.5	39.1	8.4	2.8	13.9	5.5	0.7	6.1
Co	14.3	2.9	38.7	552.0	9.7	2.1	1.2	0.8	5.3
Ni	4.4	0.6	36.3	500.7	3.9	2.4	1.8	1.9	13.2
Cu	16.0	40.2	97.1	173.3	8.1	3.2	1.9	1.8	4.4
Zn	58.2	14.7	66.8	69.1	55.2	8.7	2.1	26.3	8.9
Sr	135.2	68.2	134.9	799.9	614.3	96.15	131.85	163.65	59.6
Y	20.8	26.8	31.4	26.1	16.35	30.00	13.1	18.9	32.25
Zr	74.7	77.0	40.0	48.7	29.0	64.9	22.6	29.3	35.4
Ba	99.05	11.85	18.4	86.45	238.9	12.35	43.75	39.6	8.75
Ga	11.6	9.5	12.6	13.6	10.9	10.8	6.5	8.5	16.0
Rb	5.6	0.7	1.3	1.4	13.9	0.9	1.6	2.3	1.1
Nb	2.83	2.65	3.45	4.54	1.16	1.77	6.26	4.23	15.35
Cs	0.03	0.01	0.04	0.02	0.55	0.02	0.02	0.03	0.01
La	1.74	3.82	4.14	3.88	2.59	4.58	3.04	5.03	19.37
Ce	4.94	9.54	11.04	10.10	6.79	12.11	6.39	13.27	48.24
Pr	0.80	1.28	1.68	1.45	0.79	1.74	0.63	1.43	4.89
Nd	4.52	6.69	8.86	7.95	3.73	8.78	2.12	5.43	19.20
Sm	1.84	2.40	3.09	2.74	1.21	2.87	0.75	1.48	5.02
Eu	0.70	0.66	1.14	0.94	0.39	0.51	0.18	0.02	0.94
Gd	2.29	2.80	3.76	3.09	1.67	3.32	1.04	1.62	4.56
Tb	0.49	0.60	0.76	0.64	0.35	0.67	0.25	0.35	0.89
Dy	3.24	4.02	4.96	4.11	2.44	4.66	1.83	2.44	5.55
Ho	0.62	0.76	0.94	0.77	0.50	0.88	0.36	0.49	1.00
Er	2.07	2.61	3.00	2.54	1.63	3.07	1.01	1.66	3.11
Tm	0.33	0.42	0.47	0.40	0.27	0.51	0.20	0.32	0.51
Yb	2.25	2.85	3.06	2.57	1.78	3.53	1.26	2.22	3.31
Lu	0.36	0.46	0.47	0.39	0.28	0.59	0.17	0.37	0.51
Hf	1.80	1.86	0.94	1.14	0.91	2.06	0.57	1.13	0.78
Ta	0.13	0.11	0.22	0.18	0.08	0.15	0.51	0.39	1.06
Pb	2.59	2.25	1.73	1.27	3.01	1.20	0.27	2.58	13.46
Th	2.16	5.19	1.54	1.08	0.77	1.40	1.80	3.00	8.36
U	0.17	0.43	0.20	0.25	0.16	0.55	0.72	0.73	1.98

indistinguishable from back arc basin (Supra-subduction) plagiogranites (Pearce et al., 1984). Low TiO₂ contents (0.03 wt. %) and Nb depletion in plagiogranite dyke samples of the Zhub ophiolite indicate a back-arc setting. The Zhub ophiolite dolerite dykes' rocks are transitional between island arc and mid oceanic basalt that disproves a typical mid-ocean ridge origin for these dykes. The depletion of Nb and enrichment of the LILE over the HFSE suggest the involvement of a subduction fluid component in the source region and suggest that both the felsic and mafic dykes are formed in a back-arc basin or supra-subduction zone setting.

8. Conclusions

1. The Zhub ophiolite contains plagiogranite and dolerite dykes. The felsic dykes are intruded in gabbroic bodies of ultramafic and mafic rock unit as patches, pods and intrusions. The mafic dykes crosscut the whole sequence of the ophiolite and their relationship indicates that the emplacement of the dyke swarms postdated the formation of the Zhub ophiolite.
2. The felsic plagiogranite dykes of the Zhub ophiolite are calc-alkaline oceanic plagiogranites while dolerite dykes are tholeiitic and basaltic in composition.
3. The low value of REEs and positive Eu anomaly indicates that these felsic dykes are formed by partial

melting of basic rocks under hydrous conditions. The mafic dyke swarms are derived from an undepleted mantle source.

- The enrichment of the LILE over the HFSE and the slight depletion of Nb suggest that both dyke swarms of the Zhob ophiolite are formed in a back-arc basin or supra-subduction zone setting.

Acknowledgments

This research was part of the PhD thesis project of Mr. Abdul Naeem PhD Scholar enrolled in Centre of Excellence in Mineralogy, University of Balochistan, Quetta, Pakistan. Authors are thankful for constructive comments of Dong Liu and two anonymous reviewers which improved manuscript.

Authors Contribution

All the authors have participated sufficiently in the intellectual content, conception, and design of this work or the analysis and interpretation of the data (when applicable), as well as the writing of the manuscript.

Availability of data and materials

The data that support the findings of this study are available from the corresponding author upon reasonable request.

Conflict of interest

The author states that there is no conflict of interest.

References

- Ahmad, Z. and Abbas, S.G. 1979. The Muslim Bagh Ophiolites. In *Geodynamics of Pakistan* (eds A. Farah and A. DeJong), pp. 243–251. Pakistan: Geological Survey of Pakistan.
- Ahmed, Z. 1991. A supra-subduction origin of the Bela ophiolite indicated by acidic rocks, Khuzdar District, Pakistan. *Acta Mineralogica Pakistanica*, 5, pp. 9–24.
- Ahmed, Z. 1993. Leucocratic rocks from the Bela ophiolite, Khuzdar District, Pakistan. In *Himalayan Tectonics* (eds P.J. Treloar and M.P. Searle). *Geological Society of London Special Publications*, 74, pp. 89–100.
- Allemann, F. 1979. Time of emplacement of the Zhob Valley ophiolite and Bela ophiolite, Balochistan (preliminary report). In *Geodynamics of Pakistan* (eds A. Farah and K.A. DeJong). *Geological Survey of Pakistan*, Quetta, pp. 213–242.
- Arndt, N.T., Coltice, N., Helmstaedt, H. and Grégoire, M. 2009. Origin of Archean subcontinental lithospheric mantle: Some petrological constraints. *Lithos*, 109, pp. 61–71.
DOI: <https://doi.org/10.1016/j.lithos.2008.10.019>
- Arth, J.G. 1979. Some trace elements in trondhjemites: Their implications for magma genesis and paleotectonic setting. In *Trondhjemites, Dacites, and Related Rocks* (ed. F. Barker). Elsevier, Amsterdam, pp. 123–132.
DOI: <https://doi.org/10.1016/B978-0-444-41765-7.50008-3>
- Ashrafi, N., Dabiri, R. and Jahangiri, A. 2024. Some chemical variations in biotite, phlogopite, and muscovite, considering their tectonic setting. *Geopersia*, 14(2), pp. 307–332.
DOI: <https://doi.org/10.22059/geope.2024.373882.648749>
- Barker, F. 1979. Trondhjemites: Definition, environment and hypothesis of origin. In *Trondhjemites, Dacites, and Related Rocks* (ed. F. Barker). Elsevier, Amsterdam, pp. 1–12.
DOI: <https://doi.org/10.1016/B978-0-444-41765-7.50006-X>
- Beccaluva, L., Chinchilla-Chaves, A.L., Coltorti, M., Giunta, G., Siena, F. and Vaccaro, C. 1999. Petrological and structural significance of the Santa Elena–Nicoya ophiolitic complex in Costa Rica and geodynamic implications. *European Journal of Mineralogy*, 11, pp. 1091–1107.
- Brophy, J.G. 2009. La–SiO₂ and Yb–SiO₂ systematics in mid-ocean ridge magmas: Implications for the origin of oceanic plagiogranite. *Contributions to Mineralogy and Petrology*, 158, pp. 99–111.
DOI: <https://doi.org/10.1007/s00410-008-0372-3>
- Brophy, J.G. and Pu, X. 2012. Rare earth element–SiO₂ systematics of mid-ocean ridge plagiogranites and host gabbros from the Fournier oceanic fragment, New Brunswick, Canada. *Contributions to Mineralogy and Petrology*, 164, pp. 191–204.
DOI: <https://doi.org/10.1007/s00410-012-0732-x>
- Cassaingeu, C. 1979. Contribution à l'étude des sutures Inde–Eurasie: la zone de suture de Khost dans le Sud-Est de l'Afghanistan. L'obduction paléocène et la tectonique tertiaire. Unpublished PhD dissertation, Montpellier, France, 145 pp.
- Coleman, R.G. and Peterman, Z.E. 1975. Oceanic plagiogranite. *Journal of Geophysical Research*, 80, pp. 1099–1108.
DOI: <https://doi.org/10.1029/JB080i008p01099>
- Cox, D., Kerr, A.C., Hastie, A.R. and Kakar, M.I. 2019. The petrogenesis of small-volume plagiogranites in the Muslim Bagh Ophiolite, northwestern Pakistan: Implications for the generation of Archean juvenile continental crust. *Geological Magazine*, 156(5), pp. 874–888.
DOI: <https://doi.org/10.1017/S0016756818000250>
- Davidson, J., Turner, S. and Plank, T. 2012. Dy/Dy*: Variations arising from mantle sources and petrogenetic processes. *Journal of Petrology*, 54, pp. 525–537.
DOI: <https://doi.org/10.1093/petrology/egs076>
- Dilek, Y. and Furnes, H. 2011. Ophiolite genesis and global tectonics: Geochemical and tectonic fingerprinting of ancient oceanic lithosphere. *Geological Society of America Bulletin*, 123, pp. 387–411.
DOI: <https://doi.org/10.1130/B30446.1>
- Dilek, Y., Thy, P., Hacker, B. and Grundvig, S. 1999. Structure and petrology of Tauride ophiolites and mafic dyke intrusions (Turkey): Implications for the Neotethyan Ocean. *Geological Society of America Bulletin*, 111, pp. 1192–1216.
DOI: [https://doi.org/10.1130/0016-7606\(1999\)111<1192:SAPOTO>2.3.CO;2](https://doi.org/10.1130/0016-7606(1999)111<1192:SAPOTO>2.3.CO;2)
- Dixon, S. and Rutherford, M.J. 1979. Plagiogranites as late-stage immiscible liquids in ophiolite and mid-ocean ridge suites: An experimental study. *Earth and Planetary Science Letters*, 45, pp. 45–60.
DOI: [https://doi.org/10.1016/0012-821X\(79\)90106-7](https://doi.org/10.1016/0012-821X(79)90106-7)
- Elmi, R., Arian, M.A., Ashja Ardalan, A. and Yazdi, A. 2025. Petrology of volcanism in the Alasht–Haraz Road of the Alborz Mountain Range, south of Amol (north of Iran). *Iranian Journal of Earth Sciences*, 17(3), pp. 1–16.
DOI: <https://doi.org/10.57647/j.ijes.2025.16800>
- France, L., Koepke, J., Ildefonse, B., Cichy, S.B. and Deschamps, F. 2010. Hydrous partial melting in the sheeted dike complex at fast spreading ridges: Experimental and natural observations. *Contributions to Mineralogy and Petrology*, 160, pp. 683–704.
DOI: <https://doi.org/10.1007/s00410-010-0502-6>

- Furnes, H. and Dilek, Y. 2017. Geochemical characterization and petrogenesis of intermediate to silicic rocks in ophiolites: A global synthesis. *Earth-Science Reviews*, 166, pp. 1–37.
DOI: <https://doi.org/10.1016/j.earscirev.2017.01.001>
- Gansser, A. 1979. Reconnaissance visits to the ophiolites in Balochistan and the Himalaya. In: Geodynamics of Pakistan (eds A. Farah and K.A. DeJong), pp. 206–209. *Geological Survey of Pakistan*.
- Gnos, E., Immenhauser, A. and Peters, T.J. 1997. Late Cretaceous/early Tertiary convergence between the Indian and Arabian plates recorded in ophiolites and related sediments. *Tectonophysics*, 271, pp. 1–19.
DOI: [https://doi.org/10.1016/S0040-1951\(96\)00249-1](https://doi.org/10.1016/S0040-1951(96)00249-1)
- Grimes, C.B., Ushikubo, T., John, B.E. and Valley, J.W. 2011. Uniformly mantle-like $\Delta^{18}\text{O}$ in zircons from oceanic plagiogranites and gabbros. *Contributions to Mineralogy and Petrology*, 161, pp. 13–33.
DOI: <https://doi.org/10.1007/s00410-010-0519-x>
- Haghparsat, M., Torshizian, H. and Dabiri, R. 2019. Assessment of heavy metals concentrations and pollution in sediments of Almejogh Ophiolite Region (North-East of Iran). *Journal of Environmental Science and Technology*, 21(483), pp. 91–105.
- Hastie, A.R., Kerr, A.C., Pearce, J.A. and Mitchell, S.F. 2007. Classification of altered volcanic island arc rocks using immobile trace elements: Development of the Th–Co discrimination diagram. *Journal of Petrology*, 48, pp. 2341–2357.
DOI: <https://doi.org/10.1093/petrology/egm062>
- Hofmann, A.W. 1997. Mantle geochemistry: The message from oceanic volcanism. *Nature*, 385, pp. 219–229.
DOI: <https://doi.org/10.1038/385219a0>
- Jenner, G.A., Dunning, G.R., Malpas, J., Brown, M. and Brace, T. 1991. Bay of Islands and Little Port complexes revisited: Age, geochemical and isotopic evidence confirm supra-subduction zone origin. *Canadian Journal of Earth Sciences*, 28, pp. 135–162.
DOI: <https://doi.org/10.1139/e91-146>
- Jones, A.G. 1960. Reconnaissance Geology of Part of West Pakistan. A Colombo Plan Cooperative Project, Government of Canada, Toronto, 550 pp.
- Kakar, M.I. 2012. Petrology, geochemistry and tectonic setting of the Muslim Bagh ophiolite, Balochistan, Pakistan. PhD Thesis (unpublished), Centre of Excellence in Mineralogy, University of Balochistan, Quetta, Pakistan.
- Kakar, M.I., Kerr, A.C., Mahmood, K., Collins, A.S., Khan, M. and McDonald, I. 2014. Supra-subduction zone tectonic setting of the Muslim Bagh ophiolite, northwestern Pakistan: Insights from geochemistry and petrology. *Lithos*, 202–203, pp. 190–206.
DOI: <https://doi.org/10.1016/j.lithos.2014.05.029>
- Kazmi, A.H. and Jan, M.Q. 1997. Geology and Tectonics of Pakistan. Graphic Publishers, Pakistan.
- Khan, M.A., Kakar, M.I., Ulrich, T., Ali, L., Kerr, A.C., Mahmood, K. and Siddiqui, R.H. 2020a. Genesis of manganese deposits in the Ali Khanzai Block of the Zhob Ophiolite, Pakistan: Inferences from geochemistry and mineralogy. *Journal of Earth Science*, 31(5), pp. 884–895.
DOI: <https://doi.org/10.1007/s12583-020-1337-3>
- Khan, M.A., Ulrich, T., Kakar, M.I., Akmaz, R.M., Siddiqui, R.H. and Ali, L. 2020b. Genesis and geotectonic setting of podiform chromitites from the Zhob Valley Ophiolite, Pakistan: Inferences from chromite composition. *Episodes*, 43(4), pp. 1030–1039.
DOI: <https://doi.org/10.18814/epiiugs/2020/020065>
- Khan, S.R. 2000. Petrology and geochemistry of a part of Waziristan Ophiolite, NW Pakistan. Unpublished PhD thesis, University of Peshawar, 253 pp.
- Khan, S.R., Jan, M.Q., Khan, M.A. and Khan, T. 2001. Geochemistry and petrogenesis of the sheeted dykes from Waziristan ophiolite, NW Pakistan and their tectonic implications. Abstract: 16th HKT Workshop, Graz, Austria. *Journal of Asian Earth Sciences*, 19(3A), p. 36.
- Klein, E.M. and Langmuir, C.H. 1987. Global correlations of ocean ridge basalt chemistry with axial depth and crustal thickness. *Journal of Geophysical Research*, 92, pp. 8089–8115.
DOI: <https://doi.org/10.1029/JB092iB08p08089>
- Koepke, J., Berndt, J., Feig, S.T. and Holtz, F. 2007. The formation of SiO_2 -rich melts within the deep oceanic crust by hydrous partial melting of gabbros. *Contributions to Mineralogy and Petrology*, 153, pp. 67–84.
DOI: <https://doi.org/10.1007/s00410-006-0135-y>
- Koepke, J., Feig, S.T., Snow, J. and Freise, M. 2004. Petrogenesis of oceanic plagiogranites by partial melting of gabbros: An experimental study. *Contributions to Mineralogy and Petrology*, 146, pp. 414–432.
DOI: <https://doi.org/10.1007/s00410-003-0511-9>
- Korenaga, J. 2013. Initiation and evolution of plate tectonics on Earth: Theories and observations. *Annual Review of Earth and Planetary Sciences*, 41, pp. 117–151.
- LeBas, M.J., LeMaitre, R.W., Streckeisen, A. and Zanettin, B. 1986. A chemical classification of volcanic rocks based on the total alkali–silica diagram. *Journal of Petrology*, 27, pp. 745–750.
DOI: <https://doi.org/10.1093/petrology/27.3.745>
- Mahmood, K., Boudier, F., Gnos, E., Monié, P. and Nicolas, A. 1995. $^{40}\text{Ar}/^{39}\text{Ar}$ dating of the emplacement of the Muslim Bagh ophiolite, Pakistan. *Tectonophysics*, 250, pp. 169–181.
DOI: [https://doi.org/10.1016/0040-1951\(95\)00017-5](https://doi.org/10.1016/0040-1951(95)00017-5)
- Middlemost, E.A. 1994. Naming materials in the magma/igneous rock system. *Earth Science Reviews*, 37, pp. 215–224.
DOI: [https://doi.org/10.1016/0012-8252\(94\)90029-9](https://doi.org/10.1016/0012-8252(94)90029-9)
- Middlemost, E. A. K., 1975. The basalt clan, *Earth Science Reviews*, 11:337–364.
DOI: [https://doi.org/10.1016/0012-8252\(75\)90039-2](https://doi.org/10.1016/0012-8252(75)90039-2)
- Mullen, E.D. 1983. $\text{MnO}/\text{TiO}_2/\text{P}_2\text{O}_5$: A minor element discriminant for basaltic rocks of oceanic environments and its implications for petrogenesis. *Earth and Planetary Science Letters*, 62(1), pp. 53–62.
DOI: [https://doi.org/10.1016/0012-821X\(83\)90070-5](https://doi.org/10.1016/0012-821X(83)90070-5)
- Naeem, A., Kakar, M.I., Siddiqui, R.H., Kerr, A.C., Jan, M.Q. and Khan, M.A. 2022. Geology and petrogenesis of gabbro from the Zhob Ophiolite, Balochistan, Pakistan. *Arabian Journal of Geosciences*, 15, 1205.
DOI: <https://doi.org/10.1007/s12517-022-10417-7>
- Naeem, A., Kerr, A.C., Kakar, M.I., Siddiqui, R.H., Khan, M.A. and Ahmed, N. 2021. Petrology and geochemistry of volcanic and volcanoclastic rocks from Zhob ophiolite, North-Western Pakistan. *Arabian Journal of Geosciences*, 14, 97.
DOI: <https://doi.org/10.1007/s12517-020-06352-0>
- Nazari, M., Arian, M.A., Solgi, A., Zareisahamieh, R. and Yazdi, A. 2023. Geochemistry and tectonomagmatic environment of Eocene volcanic rocks in the Southeastern region of Abhar, NW Iran. *Iranian Journal of Earth Sciences*, 15(4), pp. 228–247.
DOI: <https://doi.org/10.30495/ijes.2023.1956689.1746>
- Pearce, J.A. 1982. Trace element characteristics of lavas from destructive plate boundaries. In: Throp, R.S. (ed.) *Andesites: Orogenic andesites and related rocks*, pp. 525–548. John Wiley and Sons, New York.
- Pearce, J.A. 1996. A user's guide to basalt discrimination diagrams. In: Bailes, A.H. et al. (eds.) *Trace element geochemistry of volcanic rocks; applications for massive sulphides exploration, short course notes*, Geological Association of Canada, 12, pp. 79–113.

- Pearce, J.A., Alabaster, T., Scheton, A.W. and Searle, M.P. 1981. The Oman ophiolite as a Cretaceous arc-basin complex: Evidence and implications. *Philosophical Transactions of the Royal Society of London*, pp. 299–317.
DOI: <https://doi.org/10.1098/rsta.1981.0066>
- Pearce, J.A., Lippard, S.J. and Roberts, S. 1984. Characteristics and tectonic significance of supra-subduction zone ophiolites. *Geological Society of London Special Publication*, 16, pp. 74–94.
DOI: <https://doi.org/10.1144/gsl.sp.1984.016.01.06>
- Robertson, A.H. 2002. Overview of the genesis and emplacement of Mesozoic ophiolites in the Eastern Mediterranean Tethyan region. *Lithos*, 65(1), pp. 1–67.
DOI: [https://doi.org/10.1016/S0024-4937\(02\)00160-3](https://doi.org/10.1016/S0024-4937(02)00160-3)
- Robinson, P.T., Malpas, J., Dilek, Y. and Zhou, M. 2008. The significance of sheeted dike complexes in ophiolites. *Geological Society of America Today*, 18, pp. 4–10.
- Salehpour, S., Arian, M.A., Rad, A.J., Zarei Sahamieh, R. and Yazdi, A. 2025. Geochemistry and technomagmatic environment of Eocene volcanic rocks in Yuzbashi Chay region, west of Qazvin (Iran). *Iranian Journal of Earth Sciences*, 17(1), pp. 1–13.
DOI: <https://doi.org/10.57647/ijes.2025.1701.04>
- Saunders, A.D. and Tarney, J. 1991. Back-arc basins. In: Floyd, P.A. (ed.) *Oceanic Basalts*. Springer, Dordrecht.
DOI: https://doi.org/10.1007/978-94-011-3042-4_10
- Sengor, A.M.C. 1987. Mid-Mesozoic closure of Permo-Triassic Tethys and its implications. *Nature*, 279, pp. 590–593.
DOI: <https://doi.org/10.1038/279590a0>
- Shervais, J.W. 1982. Ti–V plots and the petrogenesis of modern and ophiolitic lavas. *Earth and Planetary Science Letters*, 32, pp. 114–120.
DOI: [https://doi.org/10.1016/0012-821X\(82\)90120-0](https://doi.org/10.1016/0012-821X(82)90120-0)
- Sun, S.S. and McDonough, W.F. 1989. Chemical and isotope systematics of oceanic basalts: Implications for mantle composition and processes: Magmatism in the Ocean Basins. In: Saunders, A.D. and Norry, M.J. (eds.) *Geological Society of London Special Publication*, 42, pp. 313–345.
DOI: <https://doi.org/10.1144/gsl.sp.1989.042.01.19>
- Taleblian Borojenie, H., Sheykhzakariaei, S.J., Dabiri, R. and Yazdi, A. 2025. Petrogenesis and tectonic implications of Neoproterozoic to Cenozoic A-type granitoids in NW Iran: Geochemical and tectonic constraints. *Iranian Journal of Earth Sciences*, 17(4), pp. 1–19.
DOI: <https://doi.org/10.57647/ijes.2025.16894>
- Tankut, A., Dilek, Y. and Onen, P. 1998. Petrology and geochemistry of the Neo-Tethyan volcanism as revealed in the Ankara mélange, Turkey. *Journal of Volcanology and Geothermal Research*, 85(1–4), pp. 265–284.
DOI: [https://doi.org/10.1016/S0377-0273\(98\)00059-6](https://doi.org/10.1016/S0377-0273(98)00059-6)
- Thirlwall, M.F., Graham, A.M., Arculus, R.J., Harmon, R.S. and Macpherson, C.G. 1996. Resolution of the effects of crustal assimilation, sediment subduction, and fluid transport in island arc magmas; Pb–Sr–Nd–O isotope geochemistry of Grenada, Lesser Antilles. *Geochimica et Cosmochimica Acta*, 60(23), pp. 4785–4810.
DOI: [https://doi.org/10.1016/S0016-7037\(96\)00272-4](https://doi.org/10.1016/S0016-7037(96)00272-4)
- Treloar, P.J. and Izatt, C.N. 1993. Tectonics of the Himalayan collision zone between the Indian plate and the Afghan Block; a synthesis. In: Treloar, P.J. and Searle, M.P. (eds.) *Himalayan tectonics*, pp. 69–87. *Geological Society of London Special Publication*, 74.
DOI: <https://doi.org/10.1144/gsl.sp.1993.074.01.06>
- Wanless, V.D., Perfit, M.R., Ridley, W.I. and Klein, E. 2010. Dacite petrogenesis on mid-ocean ridges: Evidence for oceanic crustal melting and assimilation. *Journal of Petrology*, 51, pp. 2377–2410.
DOI: <https://doi.org/10.1093/petrology/egq056>
- Winchester, J.A. and Floyd, P.A. 1976. Geochemical magma type discrimination, application to altered and metamorphosed basic igneous rocks. *Earth and Planetary Science Letters*, 28, pp. 459–469.
DOI: [https://doi.org/10.1016/0012-821X\(76\)90207-7](https://doi.org/10.1016/0012-821X(76)90207-7)
- Wood, D.A. 1980. The application of a Th–Hf–Ta diagram to problems of tectono-magmatic classification and to establishing the nature of crustal contamination of basaltic lavas of the British tertiary volcanic province. *Earth and Planetary Science Letters*, 50, pp. 11–30.
DOI: [https://doi.org/10.1016/0012-821X\(80\)90116-8](https://doi.org/10.1016/0012-821X(80)90116-8)
- Yazdi, A., ShahHoseini, E. and Razavi, R. 2016. AMS, a method for determining magma flow in dykes (Case study: Andesite Dyke). *Research Journal of Applied Sciences*, 11(3), pp. 62–67.
DOI: <http://doi.org/10.3923/rjasci.2016.62.67>